REPORT DOCUMENTATION PAGE

Form Approved
OMB No. 0704-0188

1. REPORT DATE *(DD-MM-YYYY)* 04-06-2003	**2. REPORT TYPE** Technical Viewgraph Presentation	**3. DATES COVERED** *(From - To)*
4. TITLE AND SUBTITLE **Usage of Multi-Axis Fiber Grating Strain Sensors to Support Nondestructive Evaluation of Composite Pressure Vessels and Adhesive Bond Lines**		**5a. CONTRACT NUMBER** **F04611-02-C-0007** **5b. GRANT NUMBER** **5c. PROGRAM ELEMENT NUMBER**
6. AUTHOR(S) Eric Udd, Steve Kreger, Sean Calvert, Marley Kunzler, Katy Davol		**5d. PROJECT NUMBER** **3005** **5e. TASK NUMBER** **02AG** **5f. WORK UNIT NUMBER**
7. PERFORMING ORGANIZATION NAME(S) AND ADDRESS(ES) Blue Road Research 376 NE 219th Avenue Gresham OR 97030		**8. PERFORMING ORGANIZATION REPORT NUMBER**
9. SPONSORING / MONITORING AGENCY NAME(S) AND ADDRESS(ES) Air Force Research Laboratory (AFMC) AFRL/PRS 5 Pollux Drive Edwards AFB CA 93524-7048		**10. SPONSOR/MONITOR'S ACRONYM(S)** **11. SPONSOR/MONITOR'S NUMBER(S)** **AFRL-PR-ED-VG-2003-149**

12. DISTRIBUTION / AVAILABILITY STATEMENT

Approved for public release; distribution unlimited.

13. SUPPLEMENTARY NOTES

For presentation in the 4th International Workshop on Structural Health Monitoring in Stanford, CA, 15-17 September 2003.

14. ABSTRACT

20030812 161

15. SUBJECT TERMS

16. SECURITY CLASSIFICATION OF:			**17. LIMITATION OF ABSTRACT**	**18. NUMBER OF PAGES**	**19a. NAME OF RESPONSIBLE PERSON** Leilani Richardson
a. REPORT **Unclassified**	**b. ABSTRACT** **Unclassified**	**c. THIS PAGE** **Unclassified**	A	45	**19b. TELEPHONE NUMBER** *(include area code)* (661) 275-5015

Standard Form 298 (Rev. 8-98)
Prescribed by ANSI Std. 239.18

Usage of Multi-Axis Fiber Grating Strain Sensors to Support Nondestructive Evaluation of Composite Parts and Adhesive Bond Lines

Eric Udd, Steve Kreger, Sean Calvert, Marley Kunzler, and Katy Davol

ABSTRACT

By writing fiber gratings into birefringent polarization preserving optical fiber two and three dimensional strain may be measured. It has been demonstrated that these multi-axis fiber grating strain sensors may be used to measure shear strain and transverse strain gradients. This paper will overview the usage of these sensors to perform nondestructive evaluation of adhesive joints and composite parts.

MULTI-AXIS FIBER GRATING STRAIN SENSORS

The capability of the axial fiber grating strain sensor can be expanded into a multi-axis strain sensor by using a special type of fiber called polarization maintaining or birefringent fiber. The birefringence in the fiber is created with a built in residual stress introduced during the fiber draw. This birefringence results in a slight change in the index of refraction along two mutually orthogonal directions (termed the polarization axes.) This creates two spectral peaks for each optical grating written into the optical fiber, one associated with each polarization axis.

For this type of fiber grating strain sensor, a single fiber grating results in two distinct spectral peaks. These peaks correspond to each of the polarization axes of the polarization preserving fiber, which differ slightly in index of refraction. When the fiber is loaded transversely, the relative index of refraction of the polarization axes of the fiber change and the net result is that the difference in wavelength between the spectral peaks changes as well. When the fiber is strained axially, the fiber elongates or compresses, changing the fiber grating spectral period and the output spectrum goes to longer or shorter wavelengths, respectively.

Blue Road Research, 376 NE 219th Ave., Gresham, OR 97030 503 667-7772 x101, Fax: 503 667-7880, email: eric@bluerr.com

Figure 1a illustrates a multi-axis grating written onto polarization preserving fiber, which is subject to uniform transverse loading. In this case, the two spectral reflection peaks, corresponding to the effective fiber gratings along each birefringent (polarization) axis, will move apart or together uniformly providing a means to measure transverse strain [1],[2],[3]. In the case where load along the transverse axis is not uniform, as shown in Figure 1b, the peak associated with the nonuniform transverse load will split [1]. The transverse strain gradient can be measured quantitatively by the spectral separation between the peaks. The portion of the grating under a fixed transverse load is reflected in the amplitude of the peak. For example, in Figure 1a the transverse load along the vertical axis is uniform. There are only two spectral peaks as a result, and their spectral separation defines the transverse load. In the case of Figure 1b, the transverse load has two values along the vertical axis, each along approximately one half of the fiber grating length. In this case, the spectral peak corresponding to the vertical axis splits. The spectral shift between these subpeaks determines the transverse load gradient. As an example, a shift of 0.1 nm would correspond to approximately 300 microstrain. The amplitudes of the two split peaks are approximately equal indicating that each of the two distinct transverse load regions are approximately equal (the amplitude of the fiber grating spectral peak indicates the fraction of the fiber grating under that load). The response of the fiber to transverse strain is approximately 1/3 of that of axial strain along the length of the fiber. As a specific example at 1300 nm, a spectral shift of 0.01 nm along the fiber axis corresponds to 10 microstrain. A peak-to-peak separation of 0.01 nm due to nonuniform transverse strain corresponds to approximately 30 microstrain for 125 micron diameter bow-tie polarization preserving fiber. In the case of the fiber grating transverse and shear strain sensors developed for usage near the rocket motor liner, the sensor structures are designed to minimize transverse strain gradients.

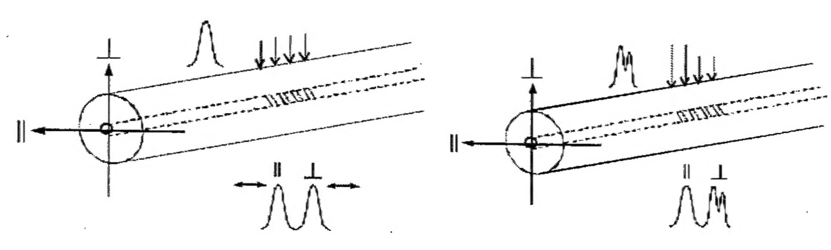

(a) **(b)**

Figure 1. The Effect of Strain on a Multi-Axis Fiber Grating

HEALTH MONITORING OF ADHESIVE JOINTS

The use of adhesive joints in aerospace structures is becoming increasingly important. From this, arises the problem of assessing joint integrity quickly, non-intrusively, accurately, and inexpensively. Current methods of assessing joint integrity, such as ultrasonics and x-rays, are time intensive and difficult to interpret. Blue Road Research's solution to monitoring adhesive joint integrity quickly and

accurately is to embed non-intrusive, multidimensional optical fiber grating strain sensors into or adjacent to the joints. As a demonstration, aluminum double lap adhesive joints were instrumented with the multi-axis sensors and subjected to tension and fatigue tests. Each specimen contained one sensor located either near the bond, embedded at the edge of the bond, or embedded towards the inner bond area. The joints with sensors embedded into the adhesive showed minimal strength degradation. The multi-axis fiber grating strain sensors were found to provide information about transverse strain, axial strain, and transverse strain gradients that can provide important information throughout the adhesive joint. By changing the orientation of the sensor, shear strain and its effects can be clearly measured.

Embedding Multi-Axis Fiber Grating Strain Sensors into Adhesive Joints

Multi-axis fiber grating strain sensors were placed interior to the joint, at the edge of the adhesive joint, and just outside the joint to simulate a retrofit. Figure 2 shows the primary locations tested. The retrofit configuration is the case where a multi-axis strain sensor was attached to an existing joint with adhesive. This provides the capability to add sensors to existing joints, not just during the fabrication of new ones.

An example of a retrofitted multi-axis fiber grating strain sensor oriented at 45 degrees to the edge of the bond is shown in Figure 3. The first chart at zero load corresponds to the spectral output of the multi-axis fiber grating strain sensor in the 1300 nm wavelength region. The two largest peaks correspond to the two transverse strain sensing axes. The smaller peaks indicate there are transverse strain gradients and the multi-axis fiber grating strain sensor is not uniformly loaded. Since the intensity of these peaks are much smaller, it indicates that these transverse gradients are very local possibly due to bubbles or impurities in the adhesive. When the adhesive joint is loaded, the two principle peaks are separated initially by a fixed spectral distance. At approximately 2400 lbs of loading, the peak to peak spectral separation of the spectral peaks increases indicating that transverse strain is increasing in the retrofitted multi-axis fiber grating sensor along its principal transverse strain sensing axis. As load is increased, transverse strain increases and is measured by increasing peak to peak separation. At about 2700 lbs of loading one of the principle peaks separates into two. This separation indicates a sudden shift in transverse loading over a portion of the grating and a degradation of the adhesive bond. The overall transverse strain continues to increase after this event until failure of the part.

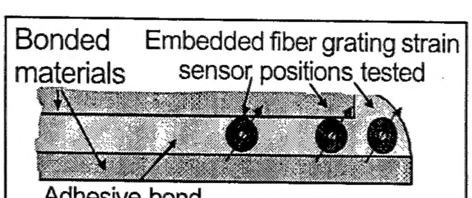

Figure 2. Multi-axis Strain Sensors Embedded into Inner (left) and Edge (middle), and Retro-fitted (right), Locations of Adhesive Bond

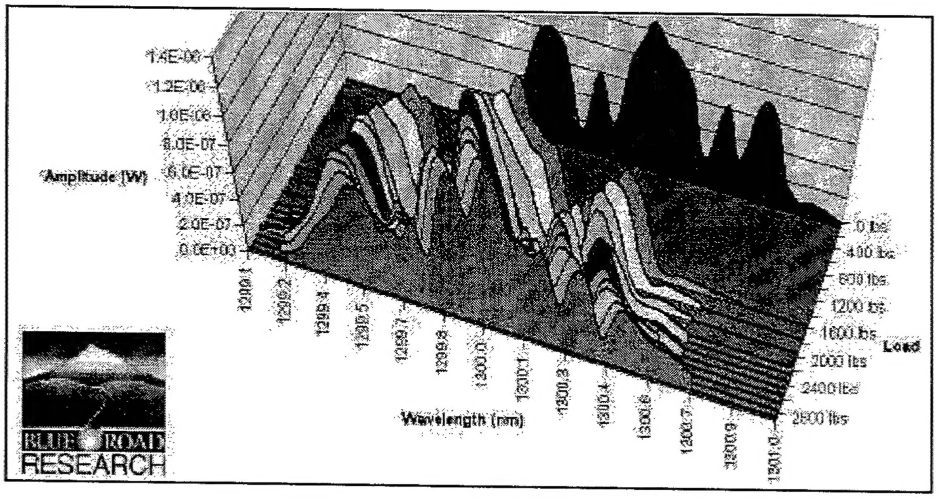

Figure 3. 1300nm Spectrum Changing with Load for Adhesive Joint Retro-Fitted with Multi-Axis Fiber Grating Strain Sensors Oriented at 45 Degrees Placed Just Beyond the Edge of the Joint (Retrofit Case)

The multi-axis fiber grating strain sensors were found to provide information about transverse strain, axial strain, and transverse strain gradients that can provide important information throughout the adhesive joint.

Applications

The main application for embedding these multi-axis strain sensors into adhesive joints is in-service health monitoring of aerospace structures where the need for lighter and more advanced configurations is increasing the use of non fixed fastener joints. Visual inspection of bonded joints cannot be performed in-service and can be time consuming, expensive, inconclusive, and in some cases not possible. It is believed that embedding these non-intrusive fiber grating shear sensors can provide critical information to the current health of an adhesive joint and be connected to other fiber grating sensors throughout the structure to form a complete structural health monitoring system.

Another application of this technology is monitoring the joint during manufacturing. Information on cure time (the strain state will change as the adhesive sets), and residual stresses can be very useful in optimizing manufacturing processes and identifying out of spec parts.

USAGE OF MULTI-AXIS FIBER GRATING STRAIN SENSORS TO DETECT DAMAGE IN A PRESSURE VESSEL

A pressure vessel was fabricated and multi-axis fiber grating strain sensors were placed to enable the detection of damage. The transverse strain axes of the multi-axis fiber grating sensors were aligned in the plane and out of the plane of the cylinder. Damage was purposefully introduced into two locations prior to cure. In

the first damage area, the prepreg tow was cut. In the second damage, area a piece of Teflon tape was introduced. The dual-axis fiber grating sensor in the area of the cut tow was able to clearly indicate that damage occurred in the plane of the cylinder after cure. In the case of the Teflon tape, the dual-axis sensor in the vicinity did not detect damage after cure but it was able to pick up damage after the first pressure cycle. Impacts were made on the pressure vessel on both the cut tow and Teflon tape damage area with resulting changes in the multi-axis strain fields that could be observed after each impact and with additional changes induced by subsequent pressure cycling.

Figure 4a shows an overview of the solid rocket motor casing demonstration article in the process of being fabricated. Figure 4b shows the placement and orientation of single and dual-axis fiber grating strain sensors. Figure 4c shows the placement of a Teflon tape defect relative to the fiber grating strain sensors in this location.

Figure 5 shows the spectral profile of the dual-axis fiber grating strain sensor placed near the area of the cut tow damage site in the pressure vessel. In this case, prepreg tow alignment elements were placed on either side of the fiber grating but not over it, so the dual-axis fiber grating was integrated directly into the composite article. Before cure and completion of the pressure vessel, the two spectral peaks corresponding to the two transverse axes of the dual-axis fiber grating strain sensor are undistorted by transverse strain gradients. The short wavelength peak is aligned in the plane of the cylinder while the long wavelength peak is orthogonal to it. After cure significant transverse strain gradients appear on the short wavelength peak corresponding to transverse strain gradients in the plane of the cylinder in the direction of the cut tow. Of the six dual-axis fiber grating strain sensors placed in the part this was the only one exhibiting this type of behavior.

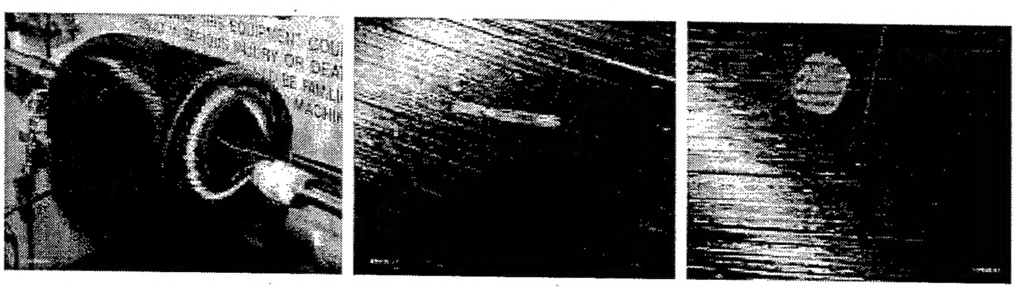

(a) (b) (c)

Figure 4. Fabrication of the Pressure Vessel Demonstration Article (a) Pressure vessel, (b) placement of dual-axis fiber grating strain sensor in prepreg tow on the first helical winding and a bare single axis fiber grating strain sensor orthogonal to it, (c) introduction of Teflon tape defect near the single and dual-axis fiber grating strain sensor.

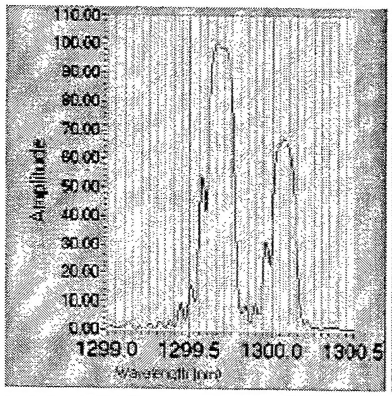

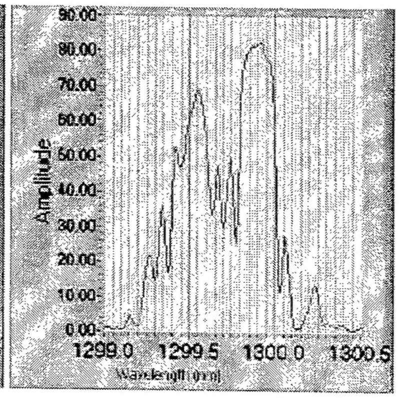

(a) (b)

Figure 5. Aligned dual-axis fiber grating strain sensor placed bare into the pressure vessel near the area of the cut tow damage site (a) before cure and (b) after cure.

Figure 6 shows the case for the dual-axis fiber grating strain sensor in a prepreg tow alignment fixture near the Teflon tape defect before and after cure. Although there is slight broadening of the spectral peaks after cure that is greater than that of dual-axis fiber grating strain sensors in the areas without defects it is much less severe than in the area of the cut tow.

Figure 7 presents data from a dual-axis fiber grating strain sensor that is located in the vicinity of the cut tow damage site. From the profile associated with Figure 5, before and after cure, it is clear that in the plane of the pressure vessel there are severe transverse strain gradients while out of the plane of the cylinder the transverse strain field is uniform. This would indicate that cutting the tow induced significant transverse strain gradients in the plane of the part. In Figures 7 and 8, the changes in the strain fields correspond to changes in the spectral profiles for the first pressure cycle before any impacts and through the third pressure cycle, which is after the impact in the region of the cut tow damage site.

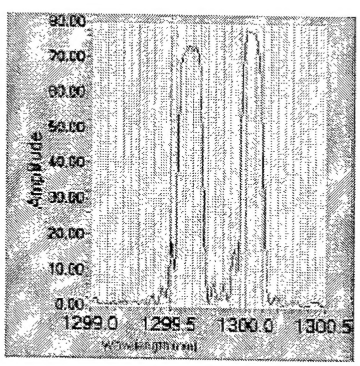

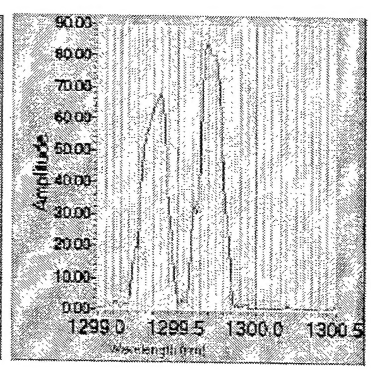

(a) (b)

Figure 6. Dual-axis fiber grating strain sensor placed in prepreg tow alignment fixture near the Teflon tape defect (a) before cure and (b) after cure.

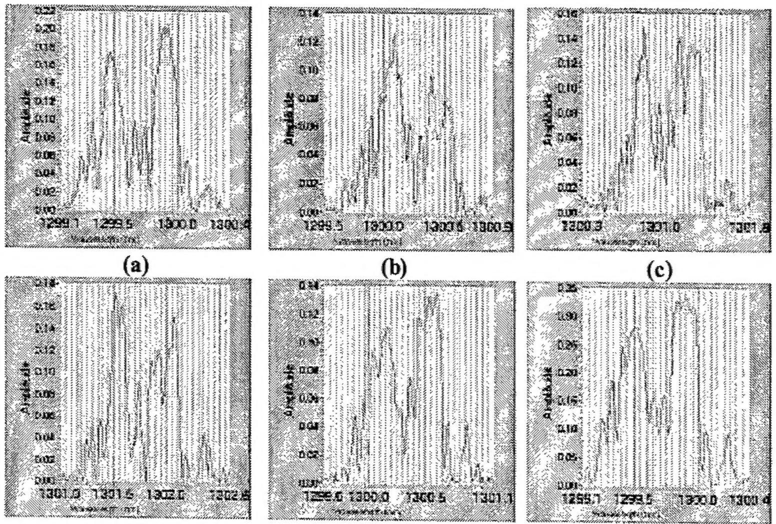

(a) (b) (c)

(d) (e) (f)

Figure 7. Spectral Profiles from Sensor 8, First Pressure Cycle Dual-axis fiber grating strain sensor near the area of the cut tow damage site during the first pressure cycle (a) 0 psi, (b) 333 psi, (c) 667 psi, (d) 1000 psi, (e) 333 psi, (f) 0 psi return.

Examining the spectral profiles of Figure 7a, the longer wavelength peak is associated with strain out of the plane of the cylindrical pressure vessel. There is a single primary peak with very few sidelobes indicating uniform transverse load in that direction. The lower wavelength peak has a series of sidelobes that indicate transverse strain gradients in the plane of the cylindrical pressure vessel. As the pressure is increased, transverse sidelobes start to appear in the out of plane strain direction. This direction is associated with longer wavelengths and becomes most severe in Figure 7d, which is associated with 1000 psi. By using a polarization controller in combination with a polarized light source the lower (in plane) and longer (out of plane) spectral profiles can be individually interrogated to clearly separate the two effects. Through the complete first pressure cycle there has been a slight overall shift in the transverse strain gradients for both the long (out of plane of the cylinder) and short (in the plane of the cylinder) wavelength peaks.

Figure 8 illustrates the third pressure cycle, which occurs after the impact in the area of the cut tow damage site. It is expected that the result of impact damage will tend to decouple the dual-axis fiber grating strain sensor from transverse strain gradients associated with the cut tow damage area. If this is the case then the lower wavelength peak should have less coupling to transverse strain gradients while the longer wavelength peak should behave in a manner similar to the earlier pressure cycle. As pressure is applied in 8b, 8c and 8d to 333, 666 and 1000 psi, the lower wavelength peak exhibits very little in the way of transverse strain gradients compared to 7b, 7c, and 7d through the same pressure range. This would indicate the impact decoupled the fiber grating strain sensor from the cut tow damage site. The longer wavelength peak however, corresponding to the out of plane axis of the cylindrical pressure vessel, continues to exhibit strong transverse strain gradients in both Figure 7 and 8, which is as expected.

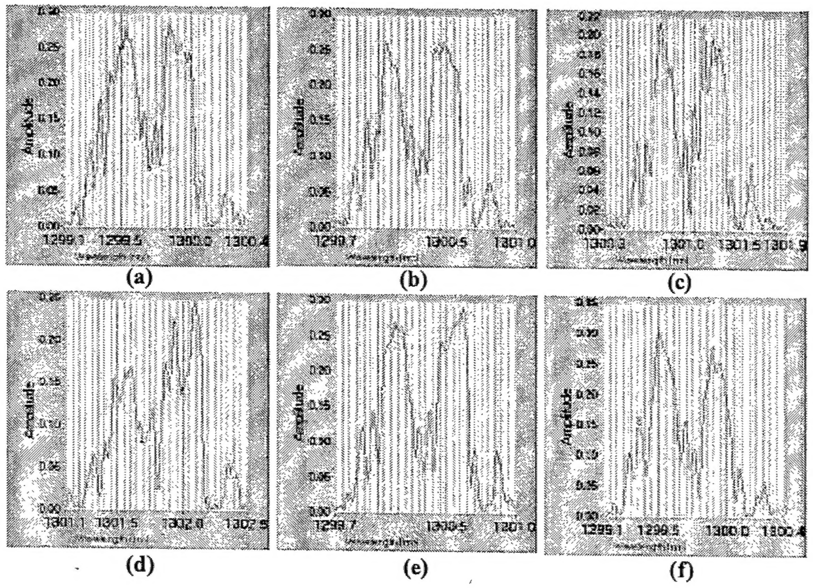

Figure 8. Spectral Profiles from Sensor 8, Third Pressure Cycle
Dual-axis fiber grating sensor approximately 2.5 cm from the cut tow damage site during the third pressure (a) 0 psi, (b) 333 psi, (c) 666 psi, (d) 1000 psi (e) 333 psi return and (f) 0 psi return.

The examples given here as background are intended to clearly demonstrate the feasibility of using single and dual-axis fiber grating strain sensors to localize and quantify the extent of damage in a cylindrical pressure vessel. A great deal of additional work is being done to use the information in these strain field changes to map our damage and correlate to results obtained from eddy current, ultrasonics, and destructive evaluation of parts.

ACKNOWLEDGEMENT

BRR gratefully acknowledges the support of the SBIR contract N68335-98-C-0122, granted by the US NAVY. Dr. Ignacio Perez of the Office of Naval Research was the Technical Contract Monitor. In addition, BRR gratefully acknowledges the support of the SBIR contract, F04611-01-C-0038, granted by Edwards AFB. Dr. Gregory Ruderman is the Technical Program Monitor.

REFERENCES

1. Perez, I., H.L. Cui, and E. Udd, "Acoustic Emission Detection using Fiber Bragg Gratings", *Proceedings of SPIE*, Vol 4328, 2001 pp. 209

2. Udd, Eric, W.L. Schulz, J.M. Seim, E. Haugse, A. Trego, P.E. Johnson, T.E. Bennett, D.V. Nelson, and A. Makino, "Multidimensional Strain Field Measurements using Fiber Optic Grating Sensors", *Proceedings of SPIE,* Vol. 3986, 2000 pp. 254

3. Schulz, Whitten, E. Udd, J.M. Seim, A. Trego, and I.M. Perez, "Progress on Monitoring of Adhesive Joints using Multi-axis Fiber Grating Sensors", *Proceedings of SPIE*, Vol. 3991, 2000 pp. 52

Usage of Multi-Axis Fiber Grating Strain Sensors to Support Nondestructive Evaluation of Composite Parts and Adhesive Bond Lines

The 4th International Workshop on
Structural Health Monitoring
Stanford University

E. Udd, S. Kreger, S. Calvert,
M. Kunzler, and K. Davol
Blue Road Research
376 NE 219th Avenue, Gresham,
Oregon 97030

Acknowledgments

This work was supported under two SBIR contracts to Blue Road Research, The adhesive joint instrumentation portion of this work was supported in part by the US NAVY contract N68335-98-C-0122. Dr. Ignacio Perez, Technical Program Monitor, and "Fiber Grating Sensor System to Determine Motor Case Damage", F04611-01-C-0038, Dr. Gregory Ruderman, Technical Program Monitor.

Blue Road Research gratefully acknowledges the support of these SBIRs, Dr. Perez and Dr. Ruderman.

BLUE ROAD RESEARCH

Fiber Optic Sensor Advantages

- Lightweight / nonobtrusive
- Passive / low power
- EMI resistant
- High sensitivity and bandwidth
- Large multiplexing potential
- Environmental ruggedness
- Complementary to telecom / optoelectronics

Unique Technologies

- Multiaxis Fiber Grating Sensors
- Transverse and Shear Strain Measurements
- High Speed Sensors/Systems (up to 10 MHz)
- Pressure, Corrosion, Environmental Sensing with very low temperature sensitivity, high multiplexing potential

Transmission and Reflection Spectra from Fiber Bragg Grating

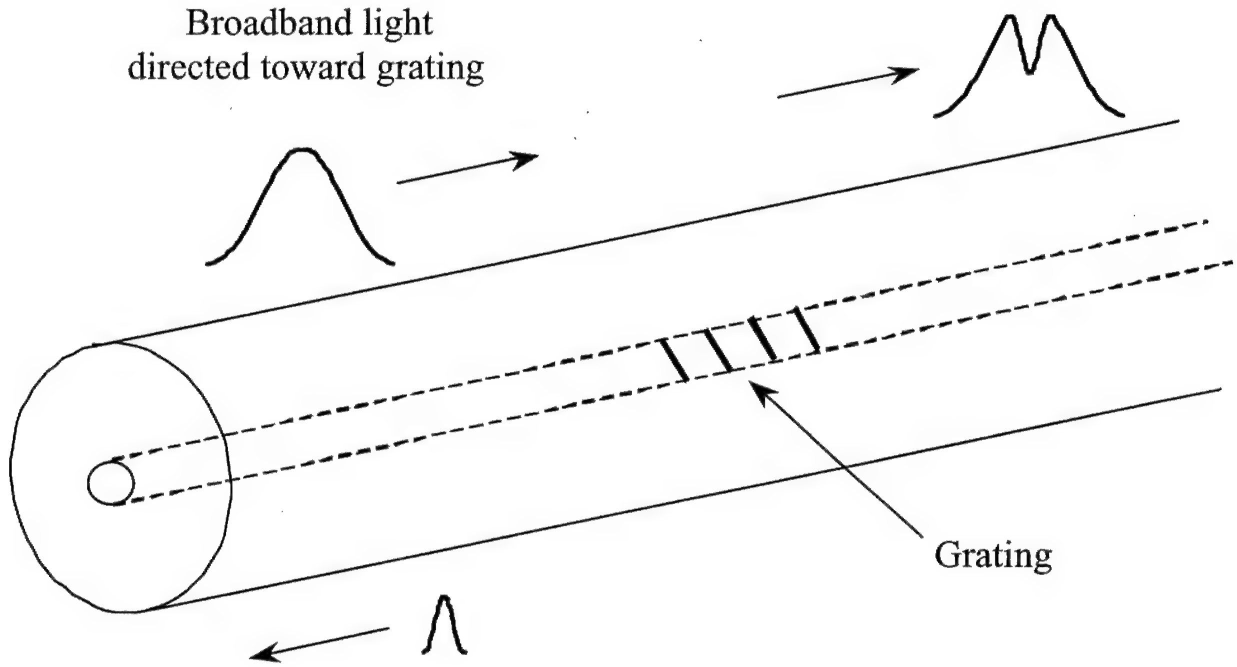

Uniform Transverse Loading

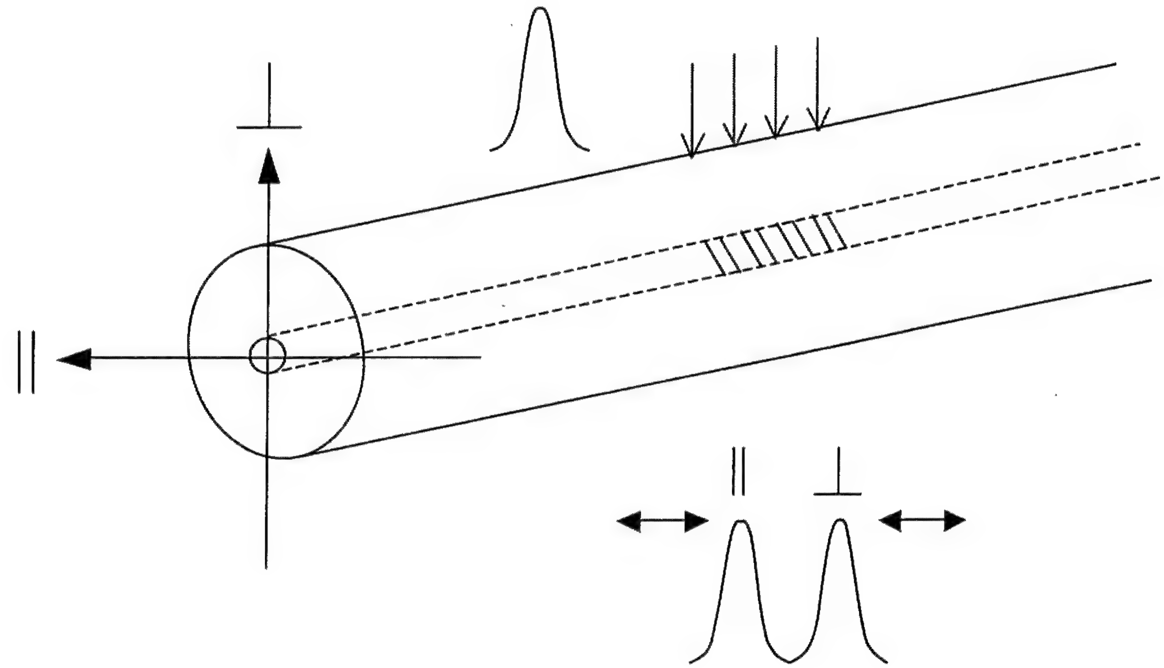

BLUE ROAD RESEARCH

Axial Loading

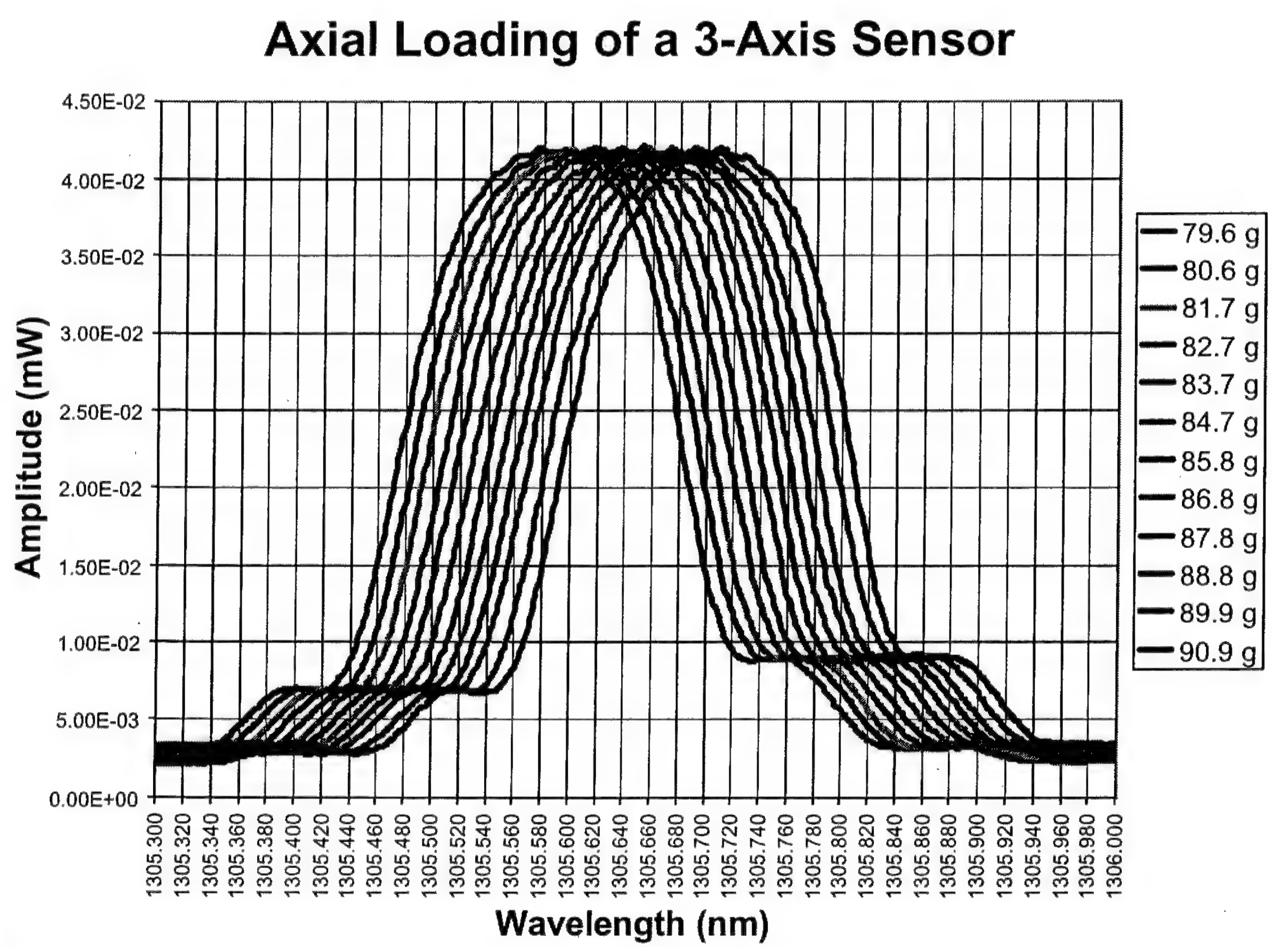

BLUE ROAD RESEARCH

7

Transverse Loading

Transverse Loading of a 3-Axis Sensor

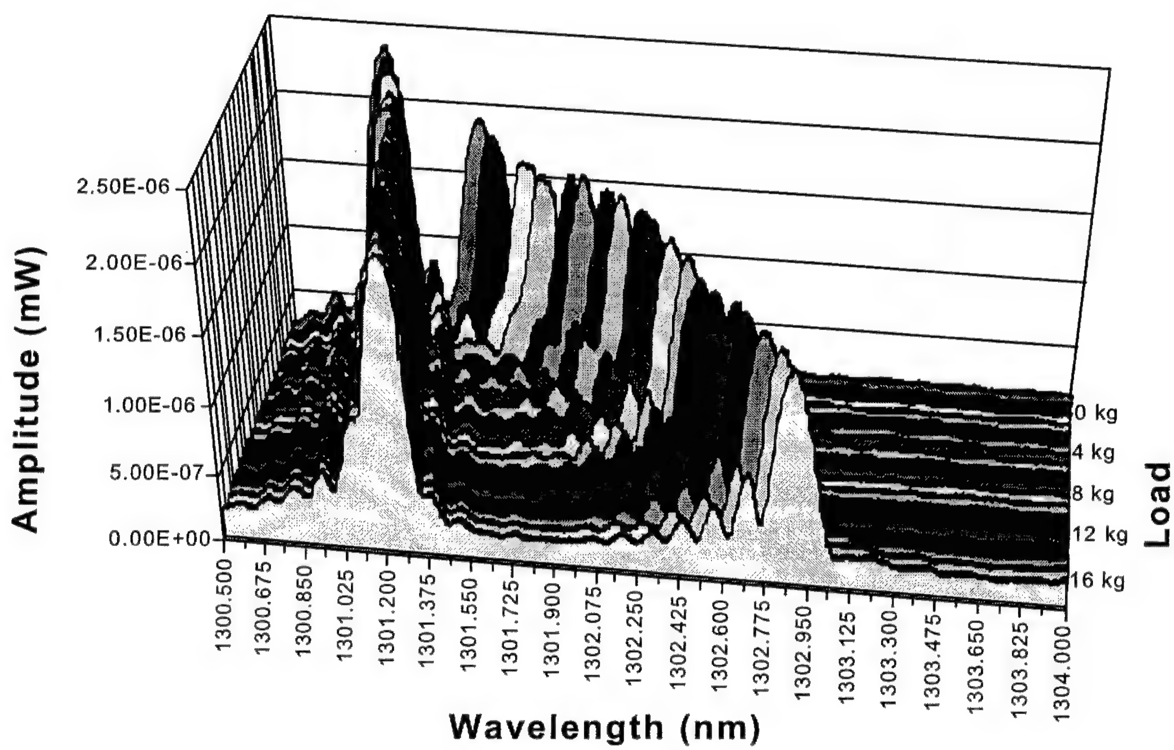

BLUE ROAD RESEARCH

Transverse Strain Gradients

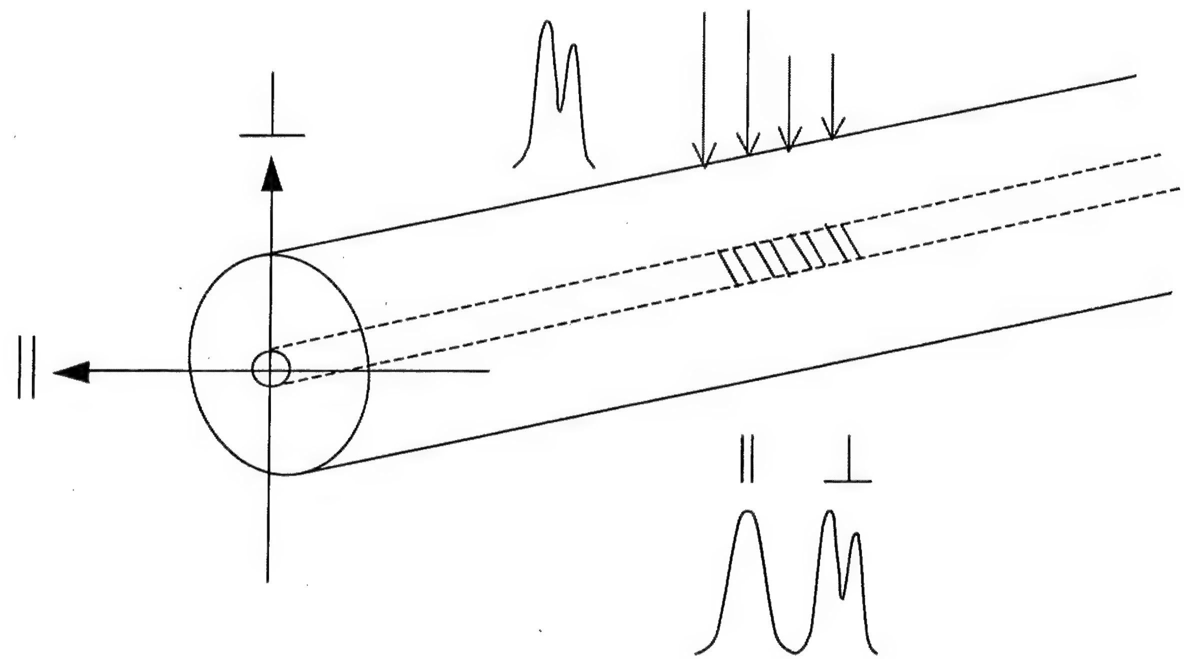

BLUE ROAD RESEARCH

Joint Health Monitoring System

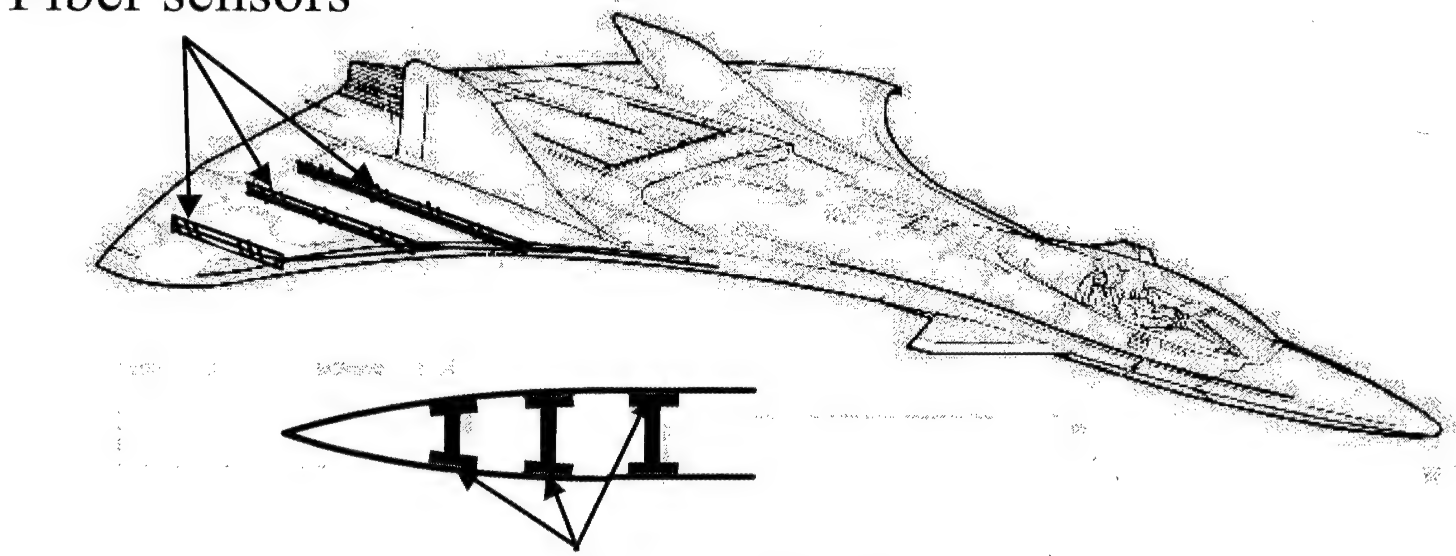

Instrumented Joint

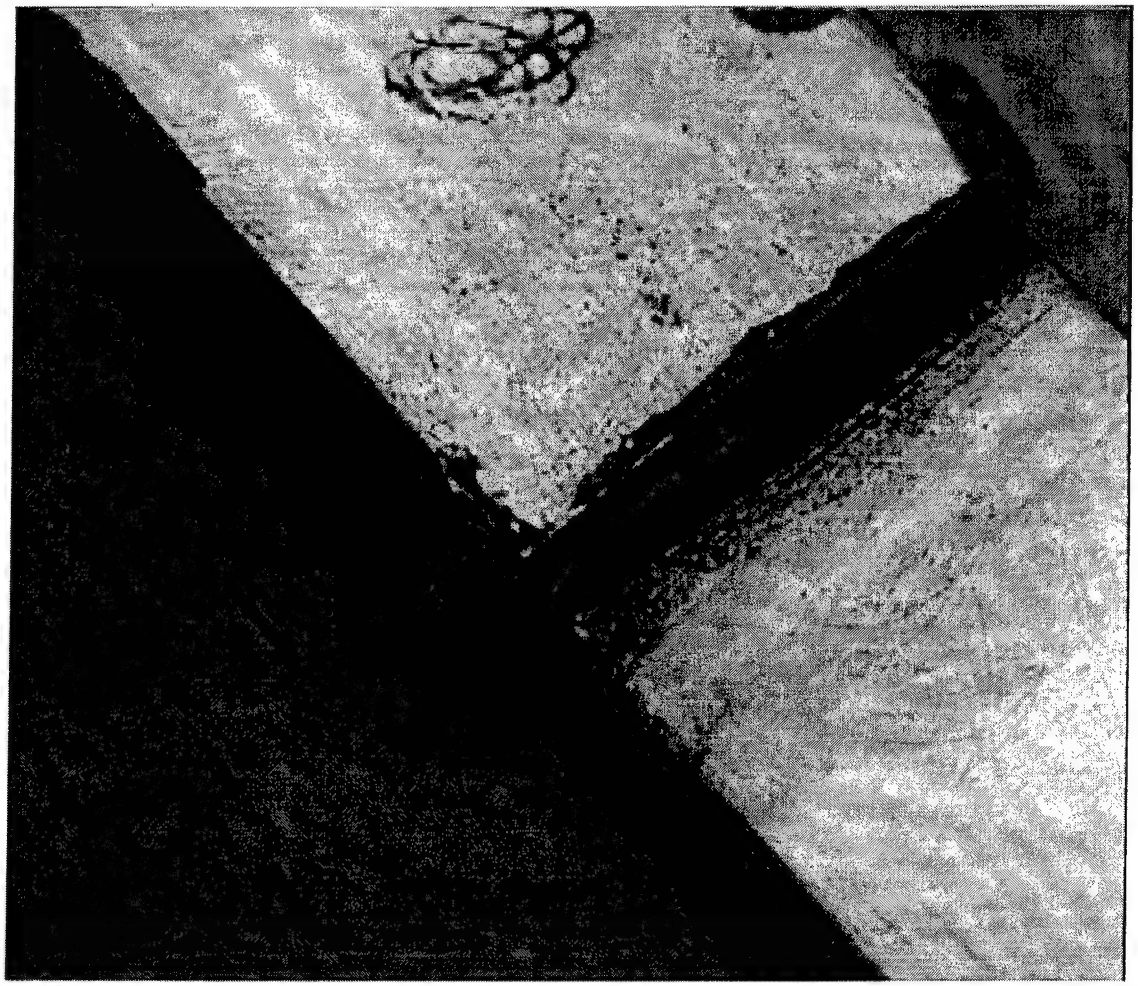

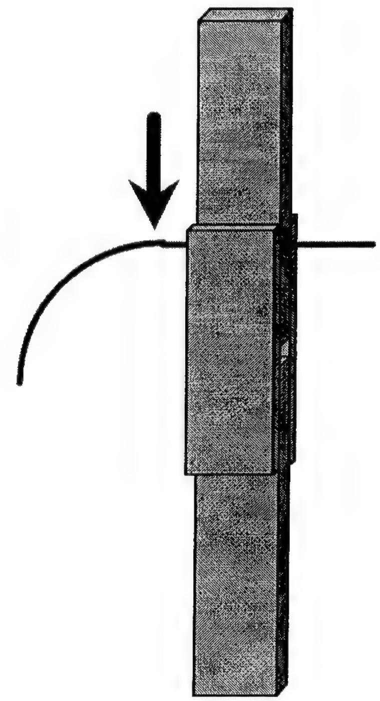

BLUE ROAD RESEARCH

Shear Strain Measurement in Adhesive Joint

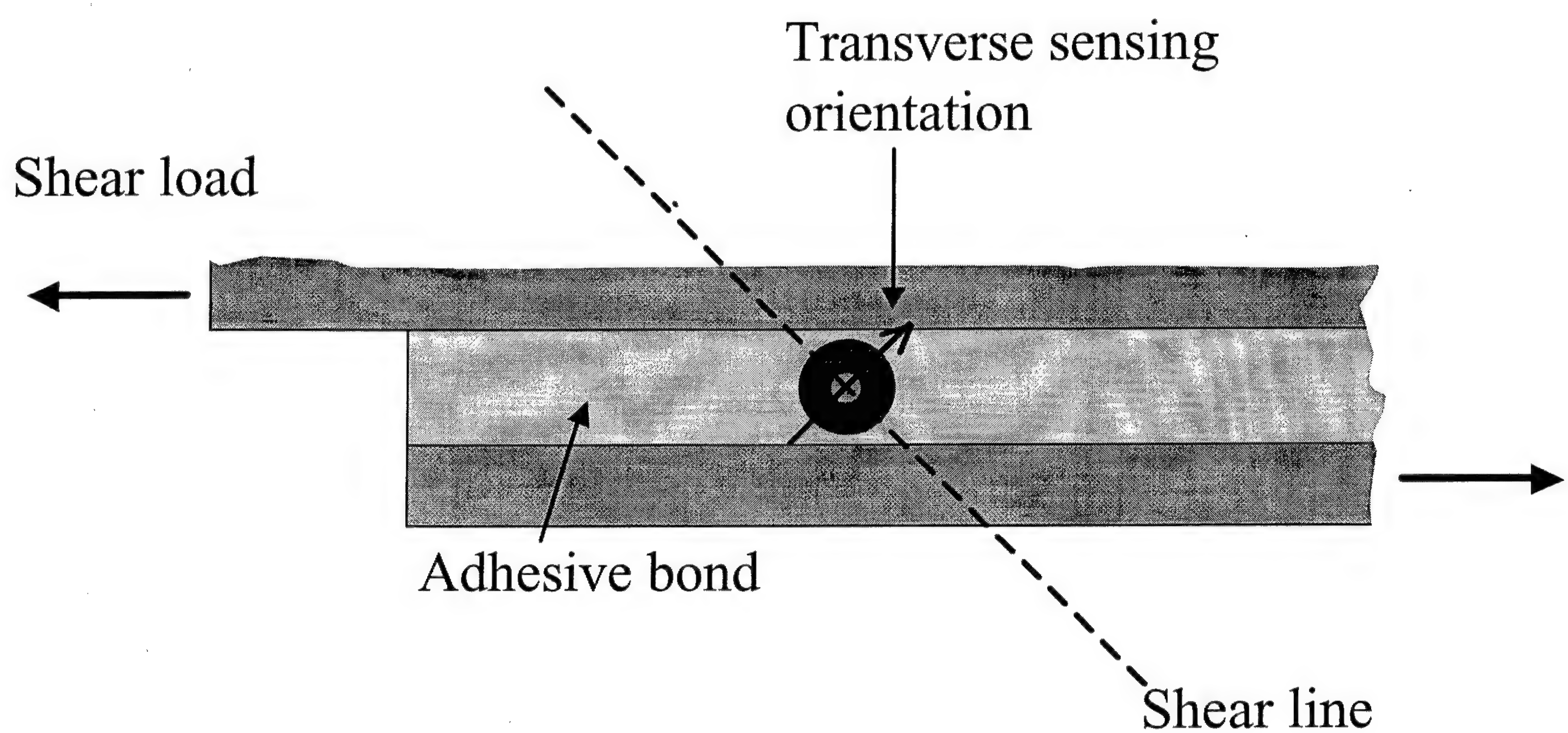

BLUE ROAD RESEARCH

Sensors embedded in, and Retro-fitted to, an Adhesive Joint

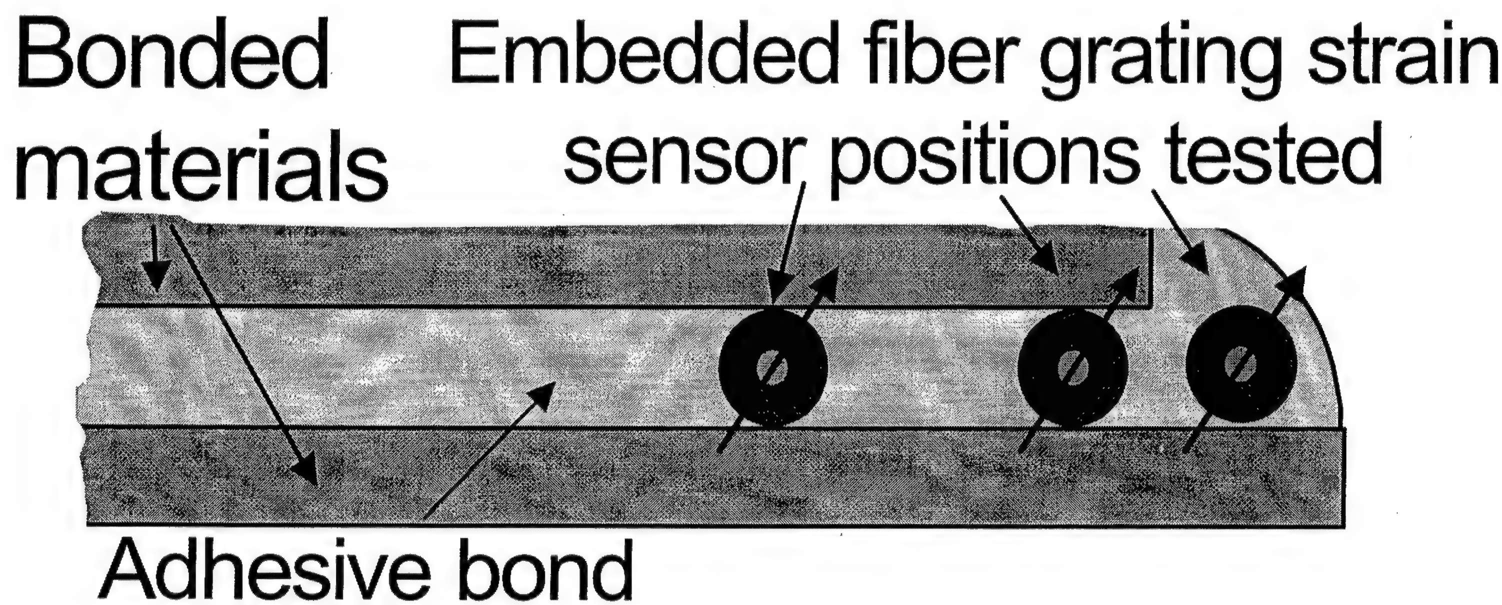

BLUE ROAD RESEARCH

Retrofit Spectral Data

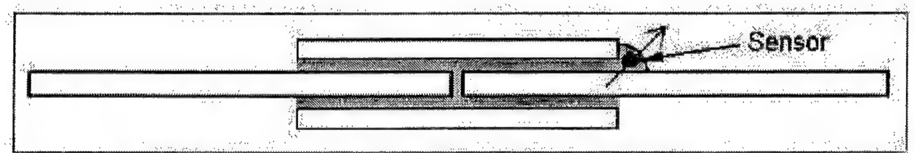

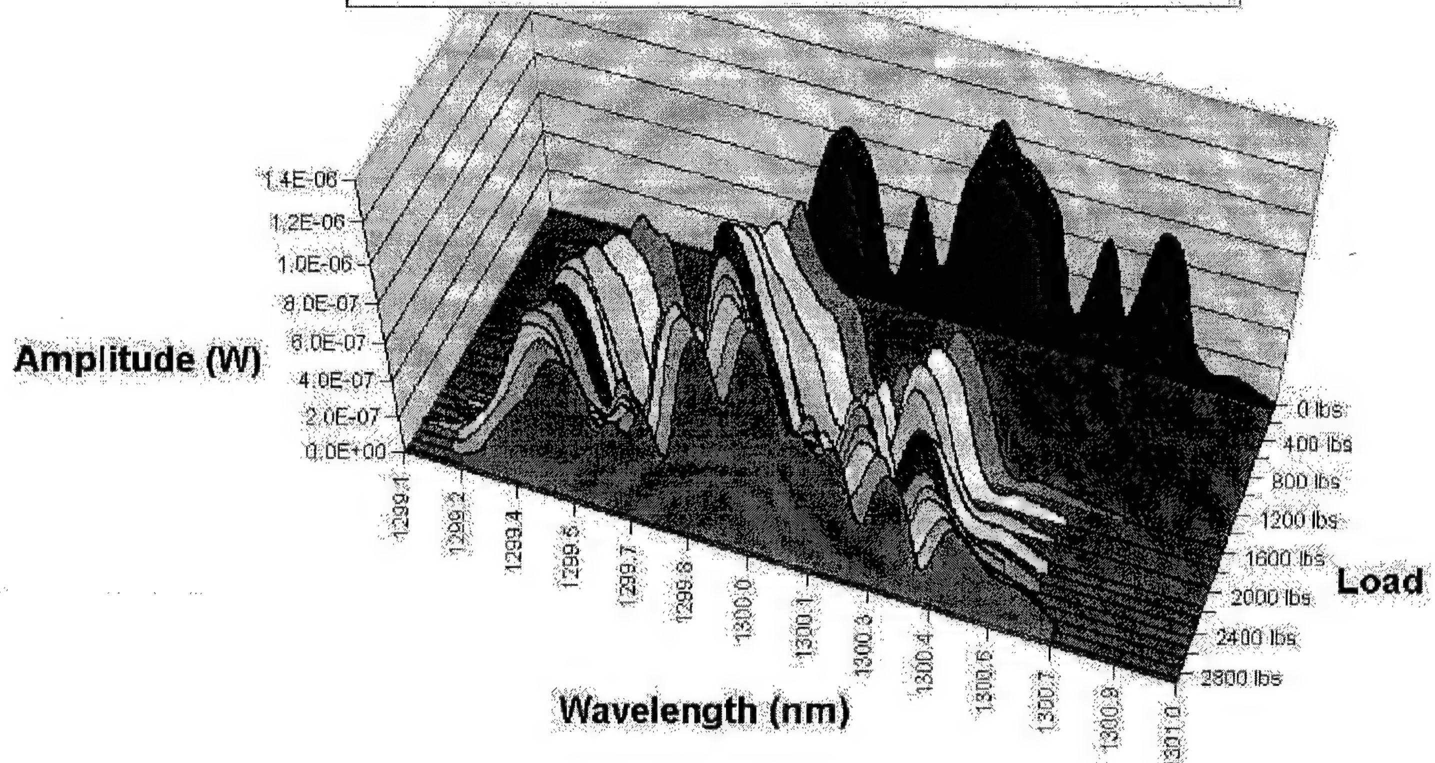

BLUE ROAD RESEARCH

Adhesive Joint Summary

- Embedded Sensors can Measure Shear Strain when the Transverse Sensing axes are Aligned with the Shear Direction

- No reduction in Part Integrity

- The Multiaxis Sensors can be Retrofit to Existing Joints and Provide Strain Information

- Strain Information from Sensors can be used to Identify the State of the Part and Predict Joint Failure.

Casing with Embedded Fiber Grating Strain Sensors

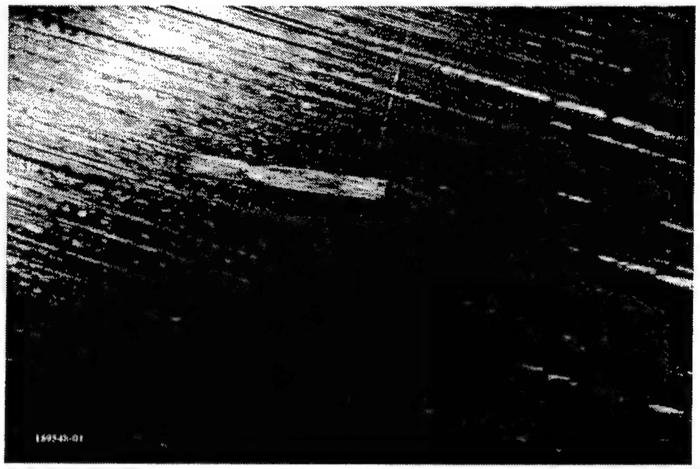

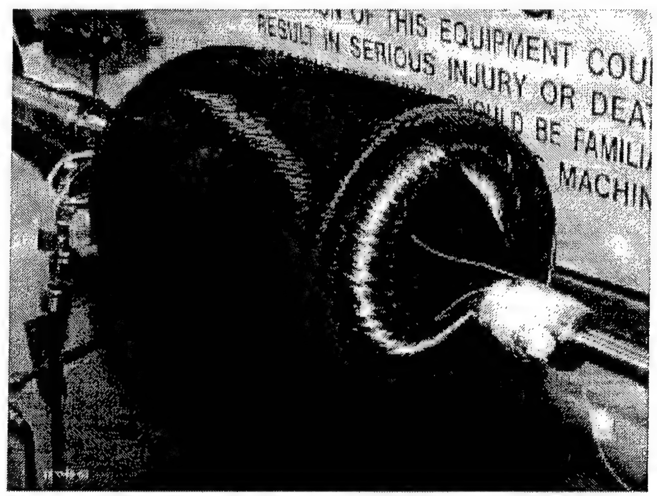

BLUE ROAD RESEARCH

Casing Cylinder Parameters

Parameter	Characteristics
Composite	T700/UF3369
Liner	Approx. 12" dia. & 20" length Cross linked Polyethylene 5.7 lbs. Made by Roto Molding of Utah
Winding Plan: Wind directly over plastic liner	3 Helical layers (0.0705 in. thick) 2 to boss -10 deg. X 1stepped back one bandwidth -16 deg. Xsb 7 hoop plies (0.0823 in. thick) 4 tows/band 5 lbs/tow tension
Winding Sequence	X O O O Xsb O O O X O

Apply internal pressure to mandrel during winding and cure.

BLUE ROAD RESEARCH

The Relative Position of Sensors #1 and #2, Which Were Placed After the First Helical Winding

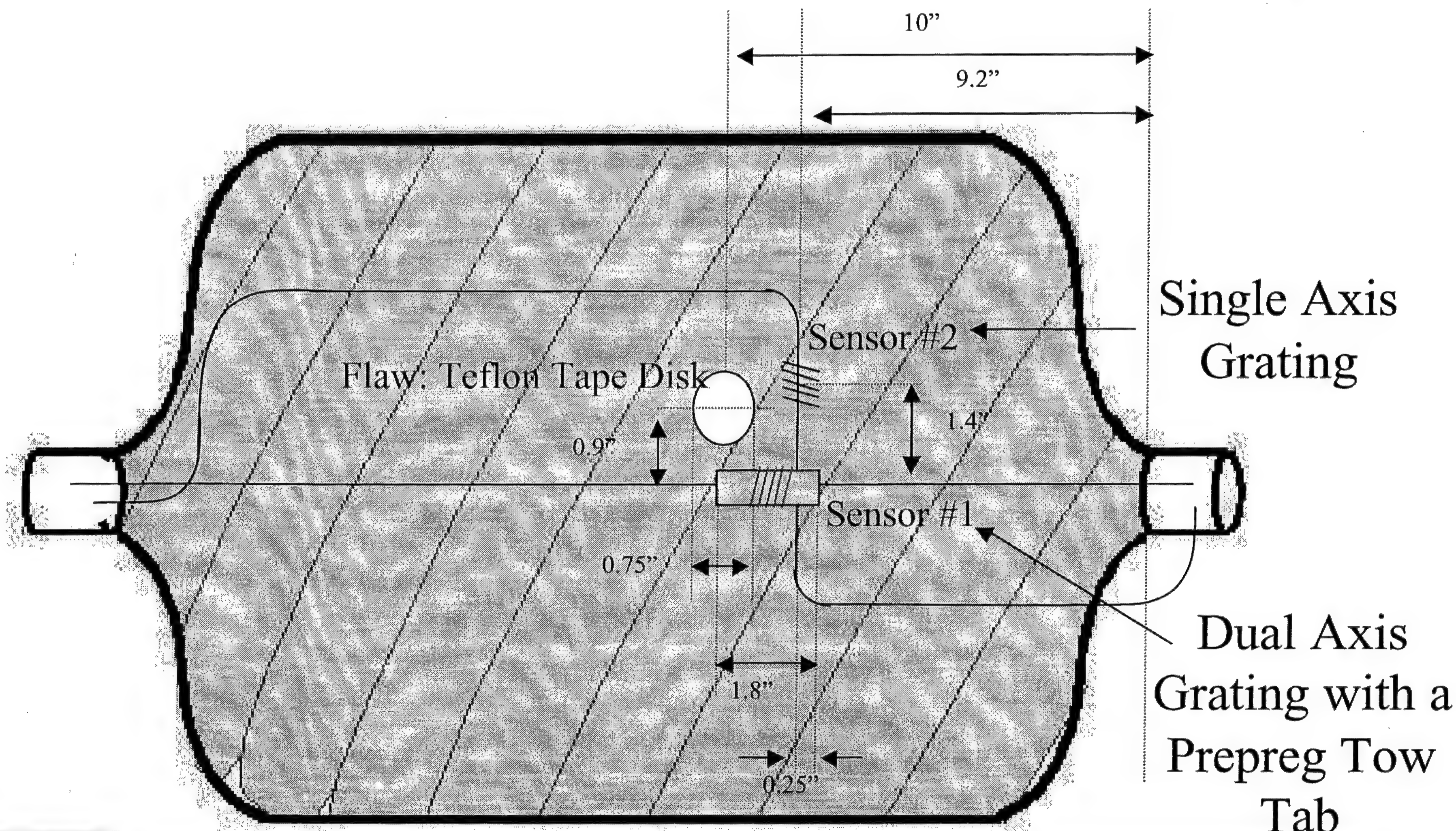

Distances Between Adjacent Sensors

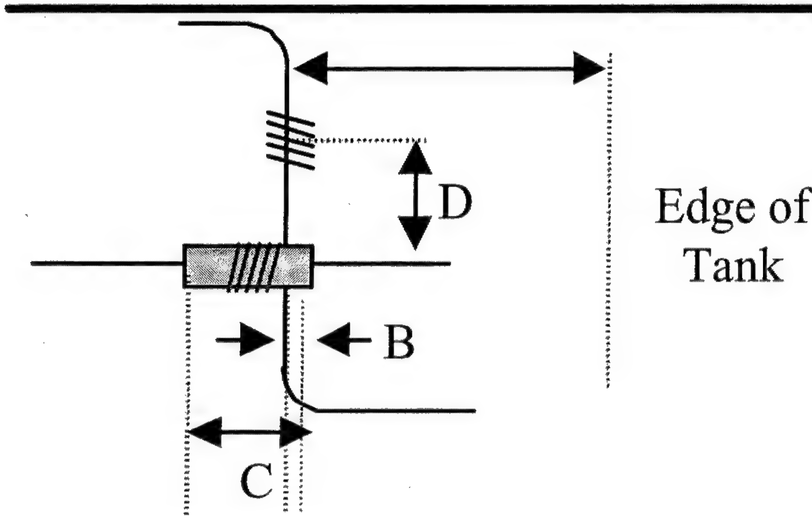

Sensor Numbers[a]	A (in.)	B (in.)	C (in.)	D (in.)
1 and 2	9.2	0.25	1.8	1.4
3 and 4	9	0.2	1.75	1.2
5 and 6	9.8	0.125	1.75	1.25
11and 12	9.5	*	*	1.75

* Not Recorded
[a] Dual Axis: Sensor #1, 4, 6 and 12
Single Axis: Sensor #2, 3, 5, and 11

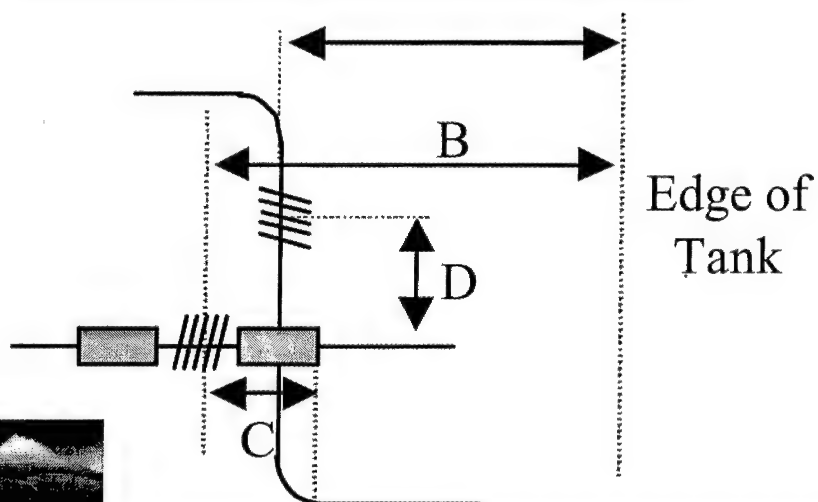

Sensor Numbers[a]	A (in.)	B (in.)	C (in.)	D (in.)
7 and 8 [b]	9.75	11	1.4	1.75
9 and 10	9.75	11.5	2	2

[a] Dual Axis: Sensor #8 and #10
Single Axis: Sensor #7 and #9
[b] Flaw: Cut 1 Band in the Subsequent Layer

BLUE ROAD RESEARCH

Phase I Demonstration Article Placed in the Pressure Test Chamber

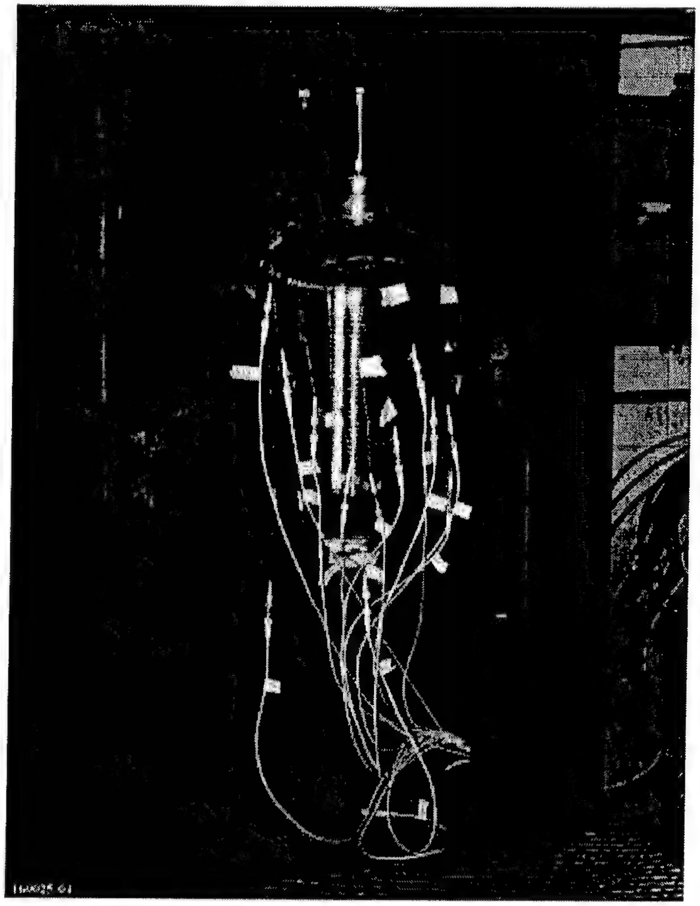

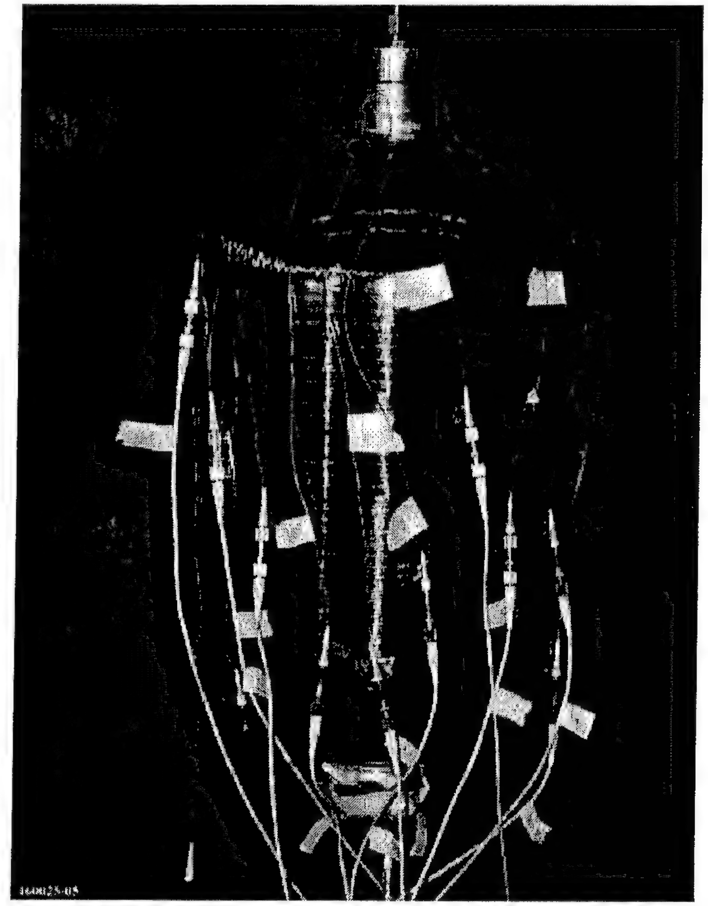

Spectral Profile of Sensor #2 (a) before and (b) after curing process

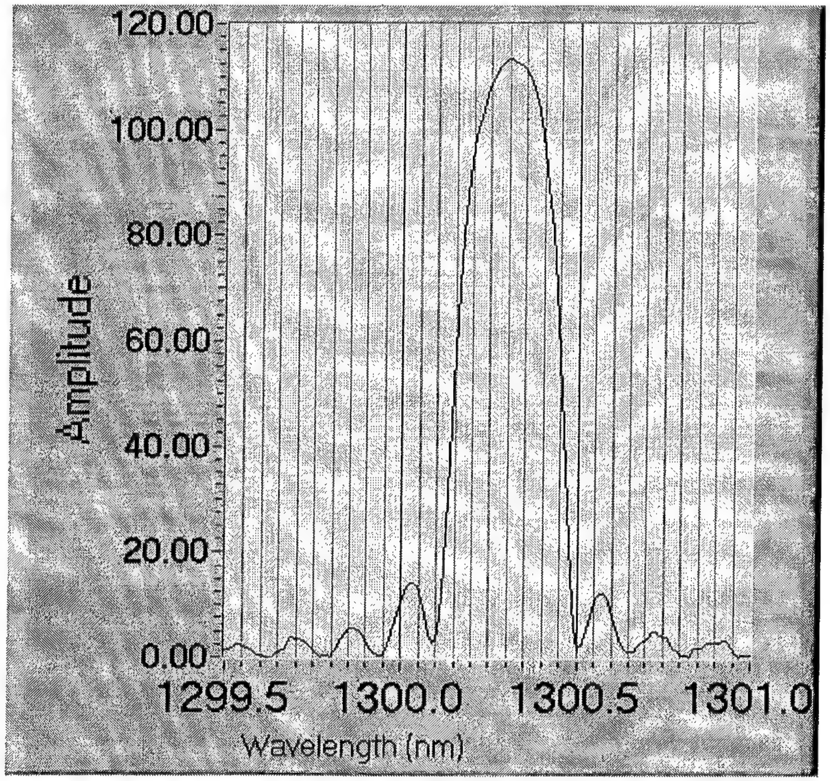

(a)

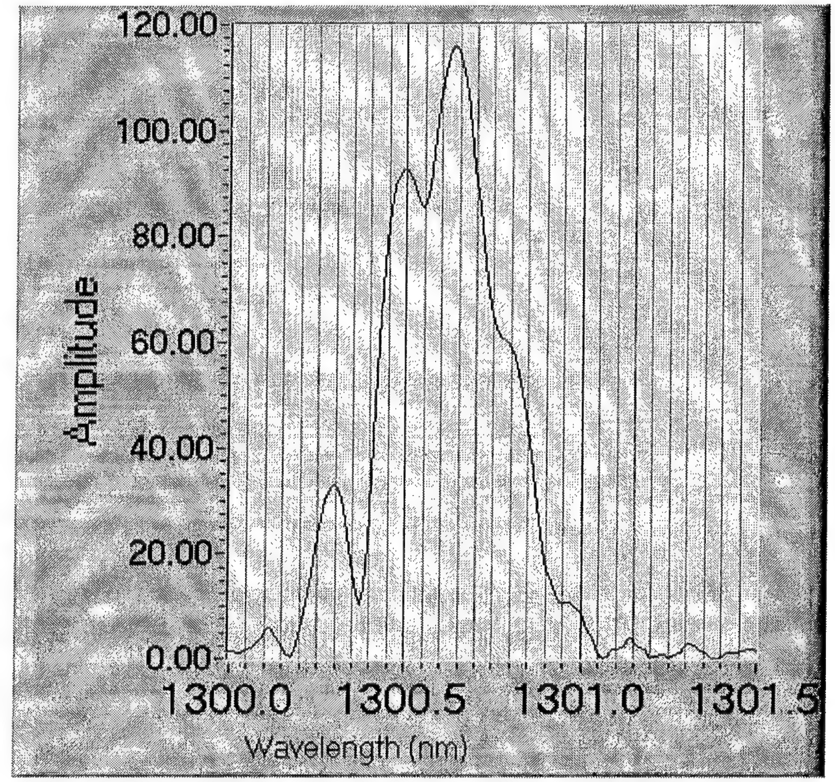

(b)

BLUE ROAD RESEARCH

Spectral Profile of Sensor #4 (a) before and (b) after curing process

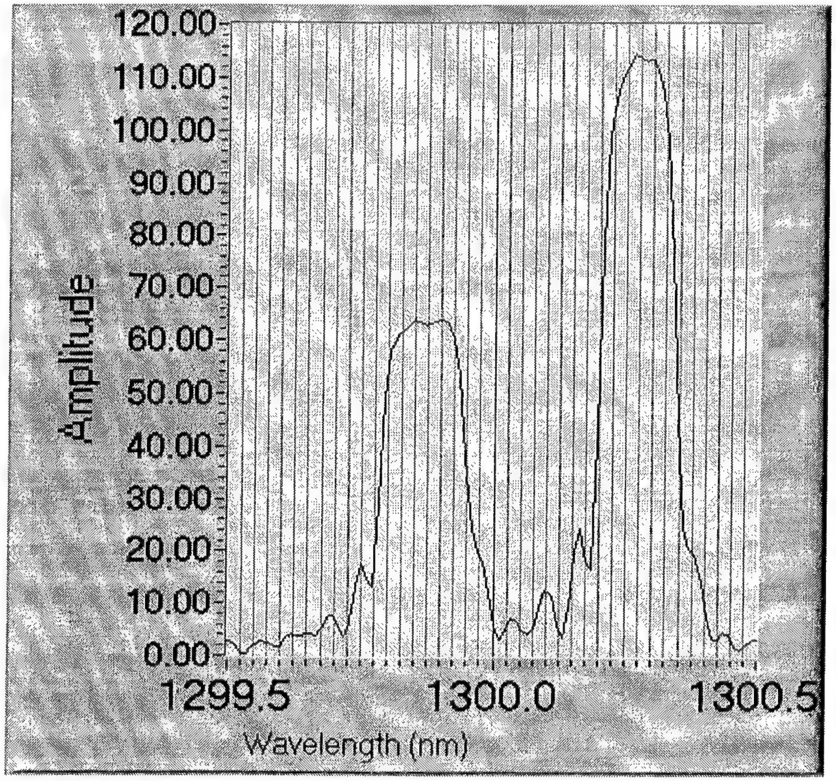

(a)

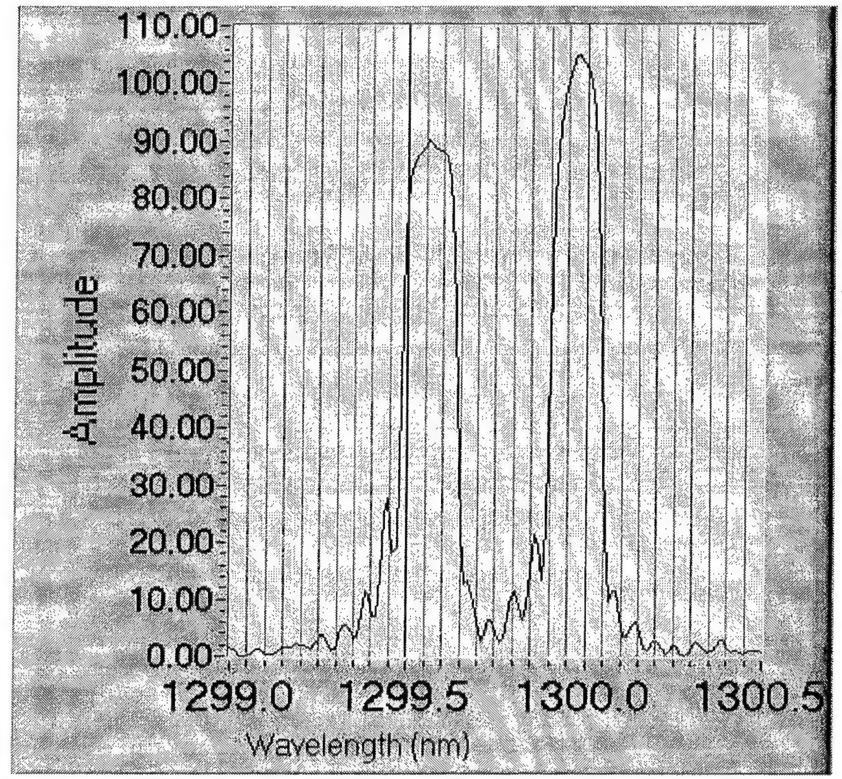

(b)

BLUE ROAD RESEARCH

Spectral Profile of Sensor #8 (a) before and (b) after curing process

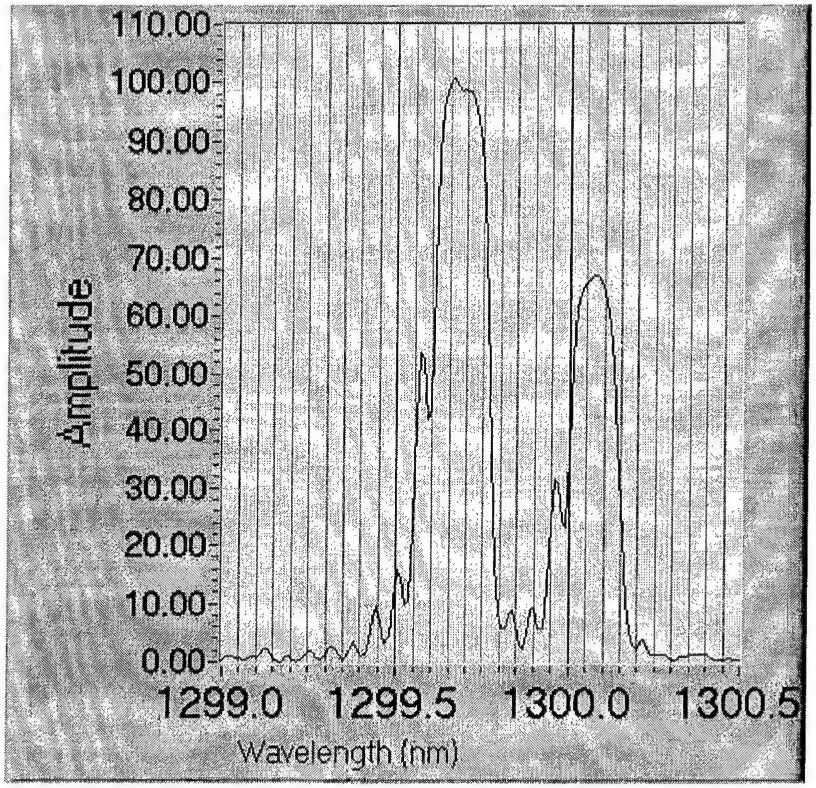

(a)

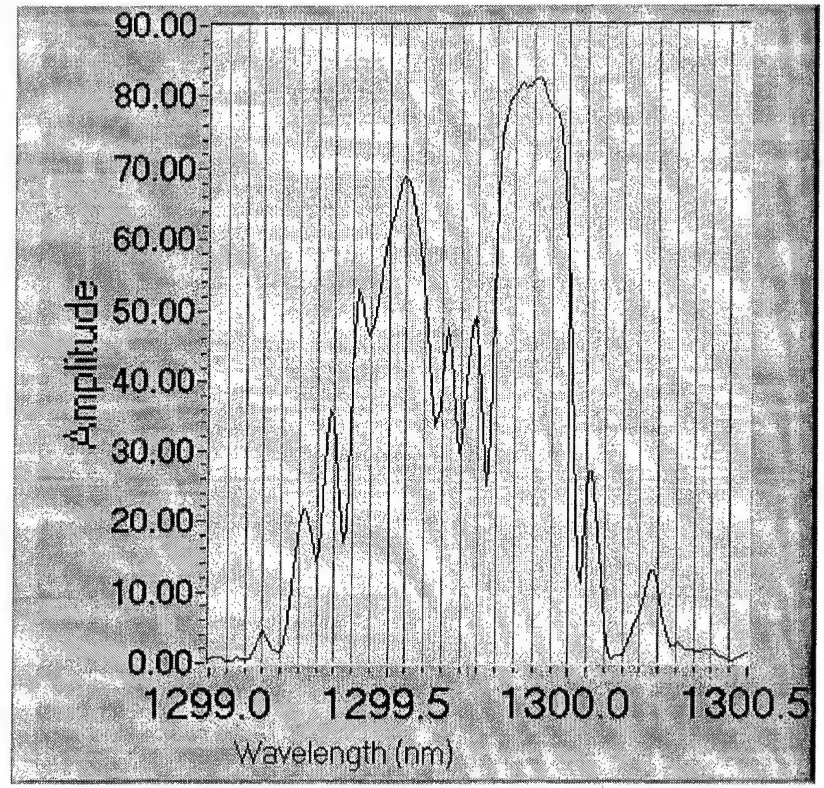

(b)

BLUE ROAD RESEARCH

Sequence of Spectral Profiles from Sensor 2 Near Teflon Tape Damage Site during 1st pressure cycle

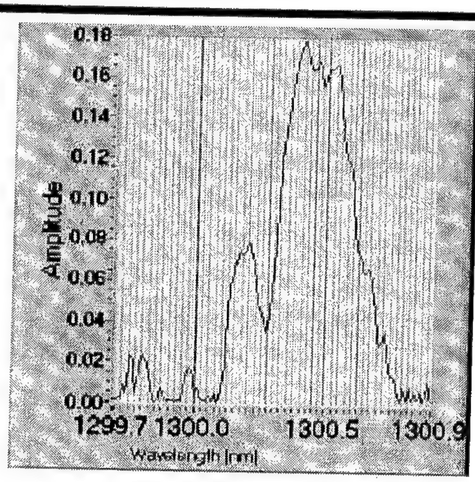

0 psi

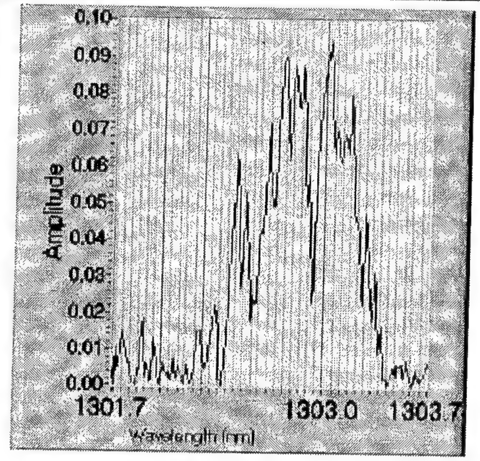

666 psi

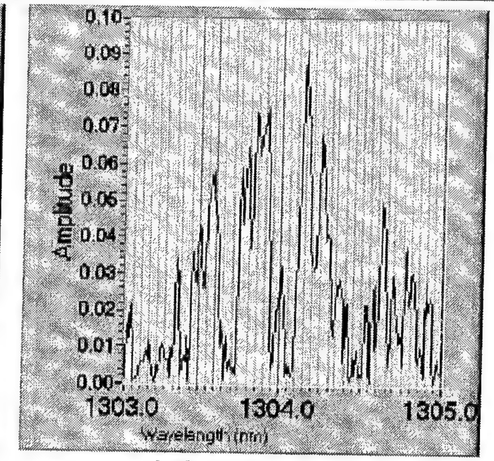

1000 psi

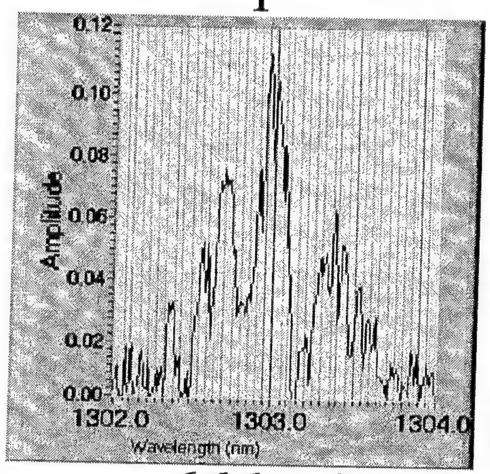

666 psi

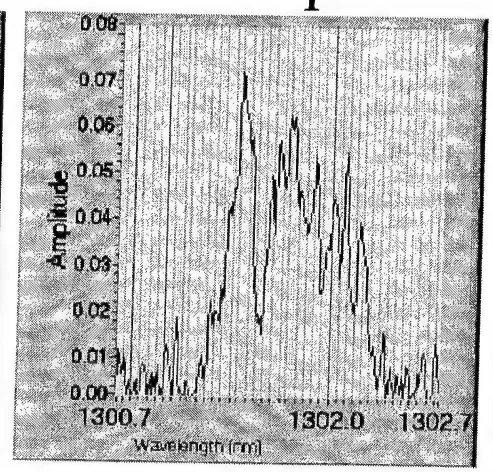

333 psi

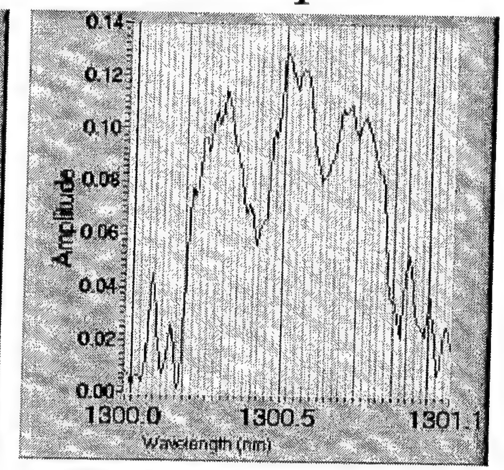

Return to 0 psi

BLUE ROAD RESEARCH

Spectral Profiles of Sensor 2 After Impact 3 Near Teflon Tape Area During 4th Pressure Cycle

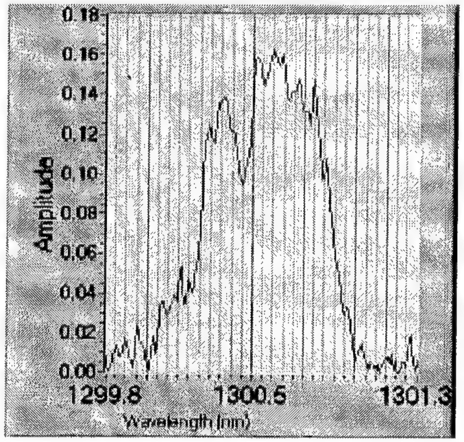

0 psi

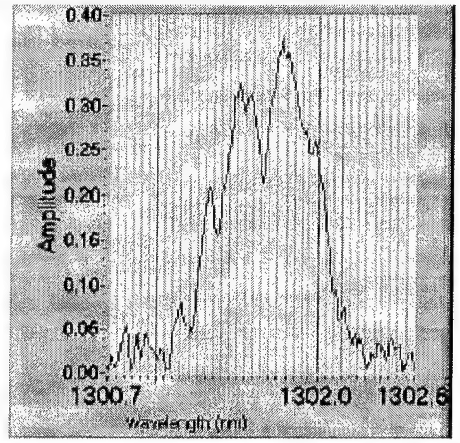

333 psi

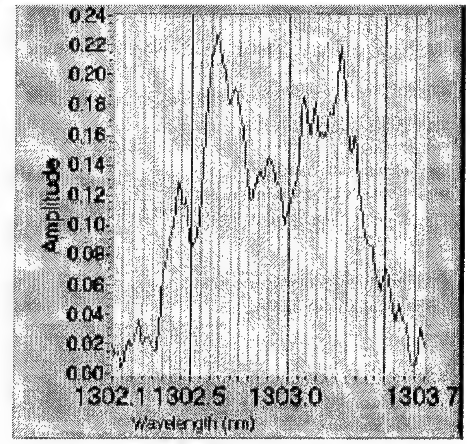

666 psi

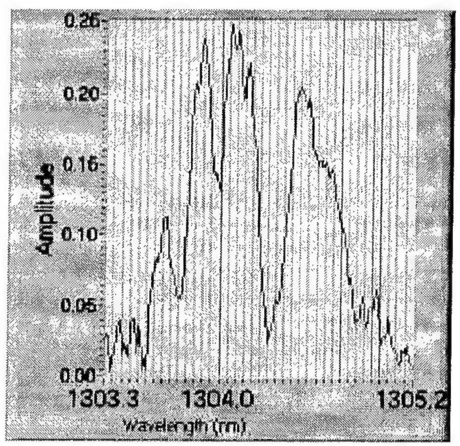

1000 psi

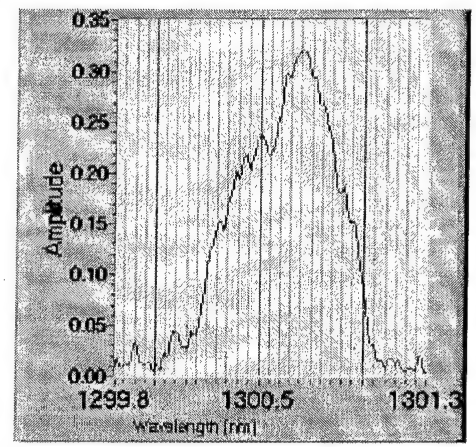

Return to 0 psi

BLUE ROAD RESEARCH

Spectral Profiles of Sensor 4 After Impact 2 During 3rd Pressure Cycle Remote From Any Damage Site

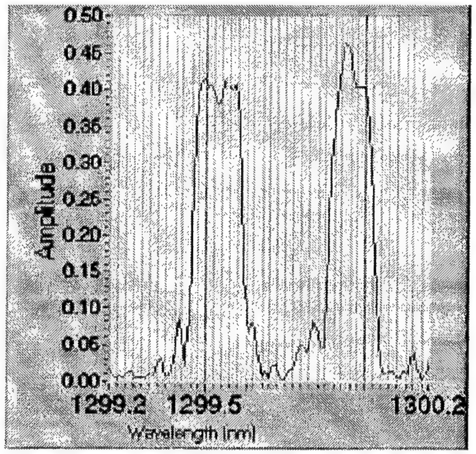

0 psi

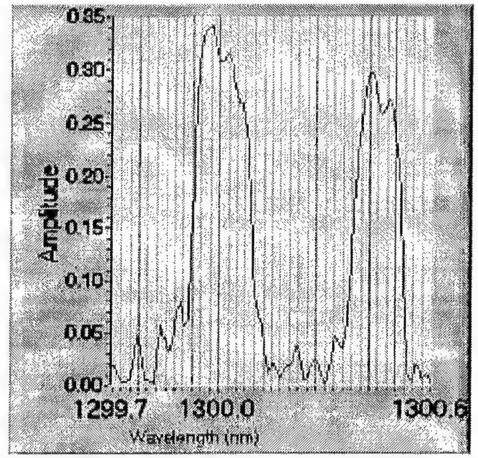

333 psi

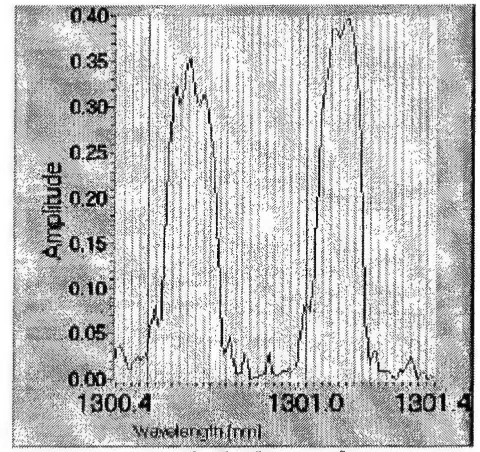

666 psi

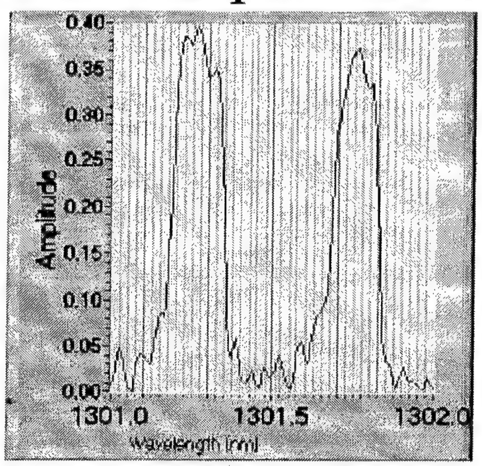

1000 psi

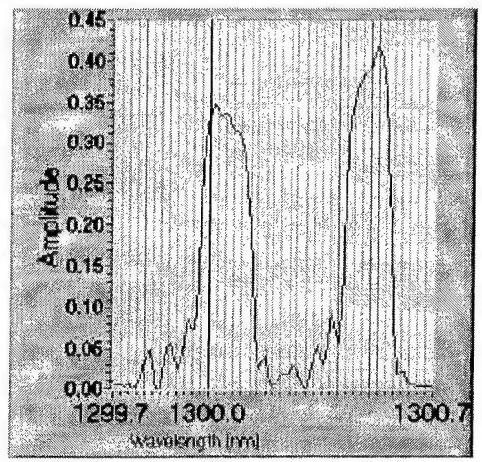

333 psi

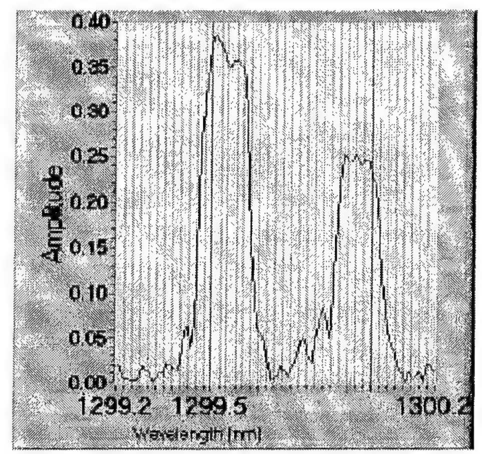

Return to 0 psi

BLUE ROAD RESEARCH

Spectral Profiles of Sensor 8 Near Cut Tow Area During 1st Pressure Cycle

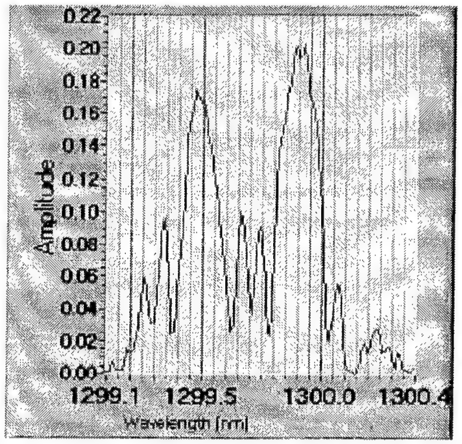

0 psi

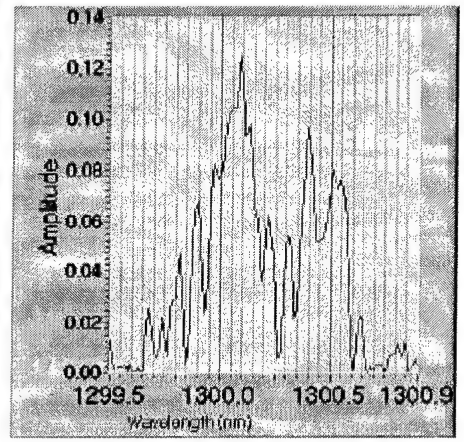

333 psi

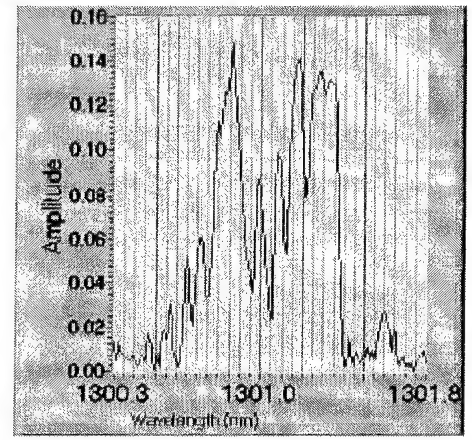

667 psi

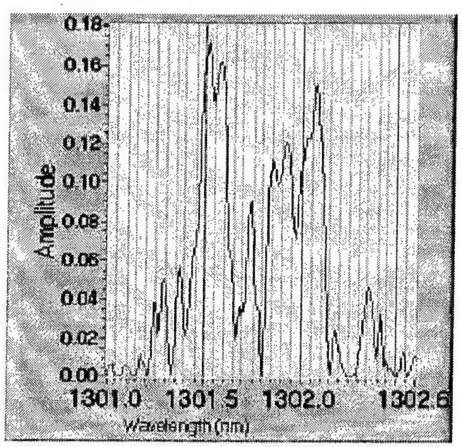

1000 psi

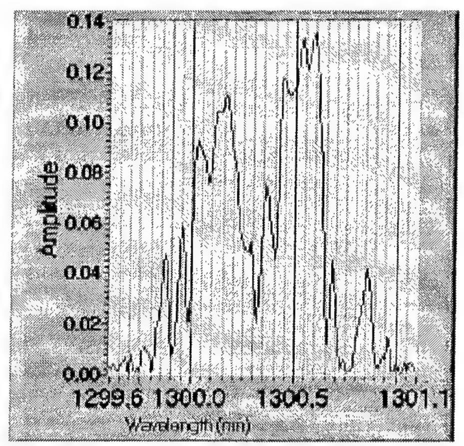

333 psi

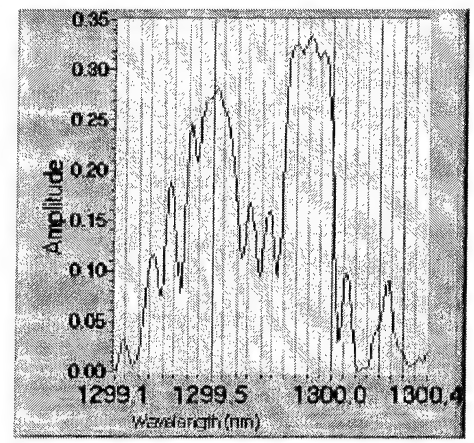

Return to 0 psi

BLUE ROAD RESEARCH

Spectral Profiles of Sensor 8 After Impact 2 Near Cut Tow Area During 3rd Pressure Cycle

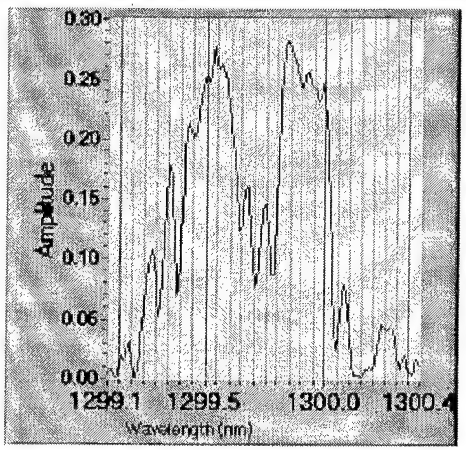

0 psi

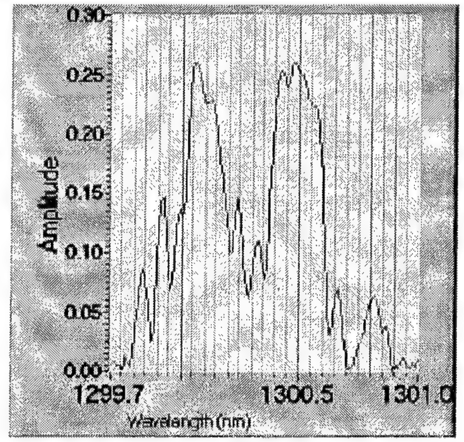

333 psi

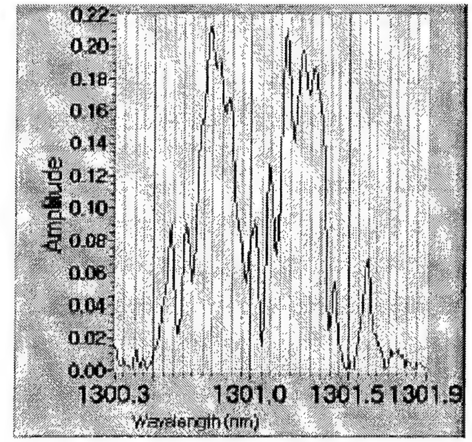

667 psi

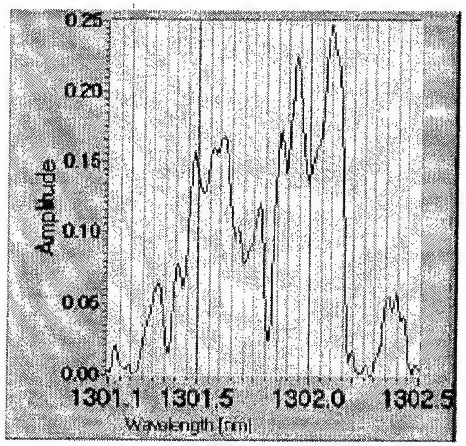

1000 psi

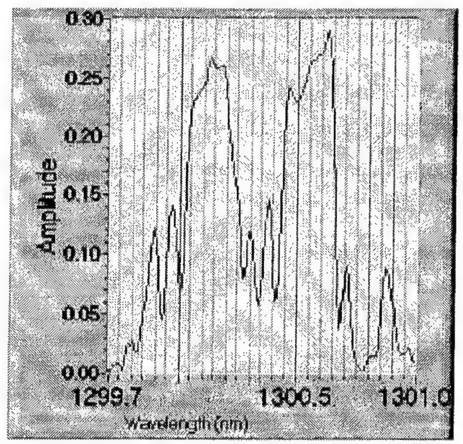

333 psi

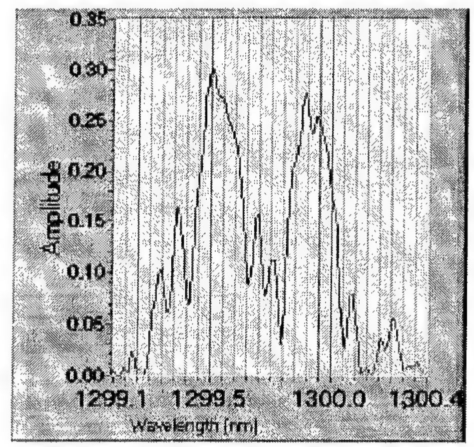

Return to 0 psi

BLUE ROAD RESEARCH

Drop Test Setup and Damage Induced

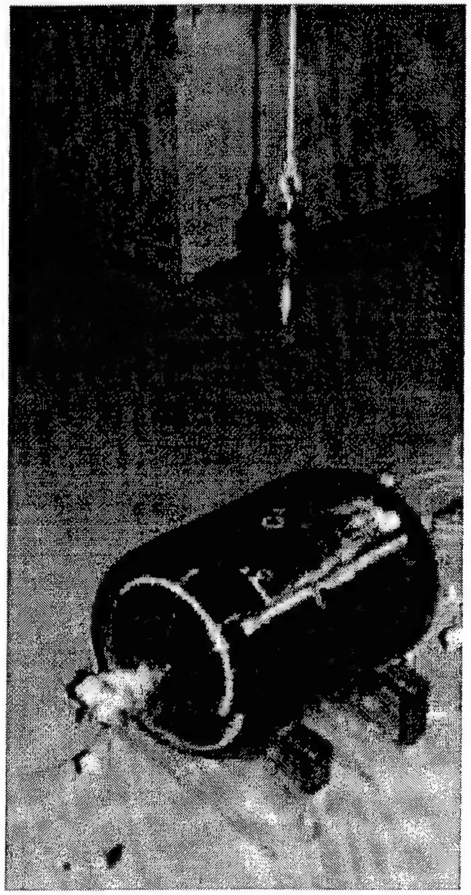

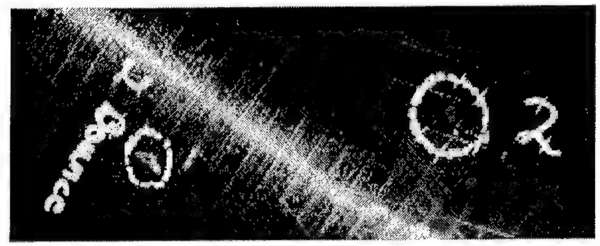

Damage induced by drop test 2 with bounce, 15 foot pound drop on 1 cm^2 area, $\approx$ 2.5 cm from sensors 7 and 8 near cut tow area

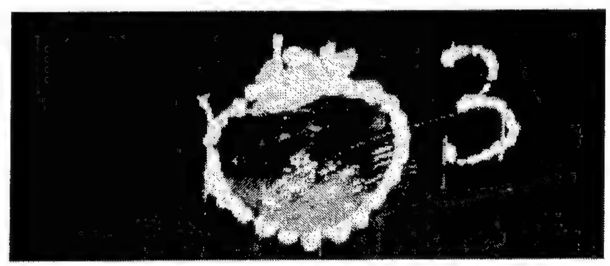

Drop test 3, a 30 foot pound drop on 1 cm^2 area $\approx$ 2.5 cm from sensors 1 and 2 near Teflon tape

BLUE ROAD RESEARCH

Cross Sectional View of Pressure Bottle Sensors and Impact Locations

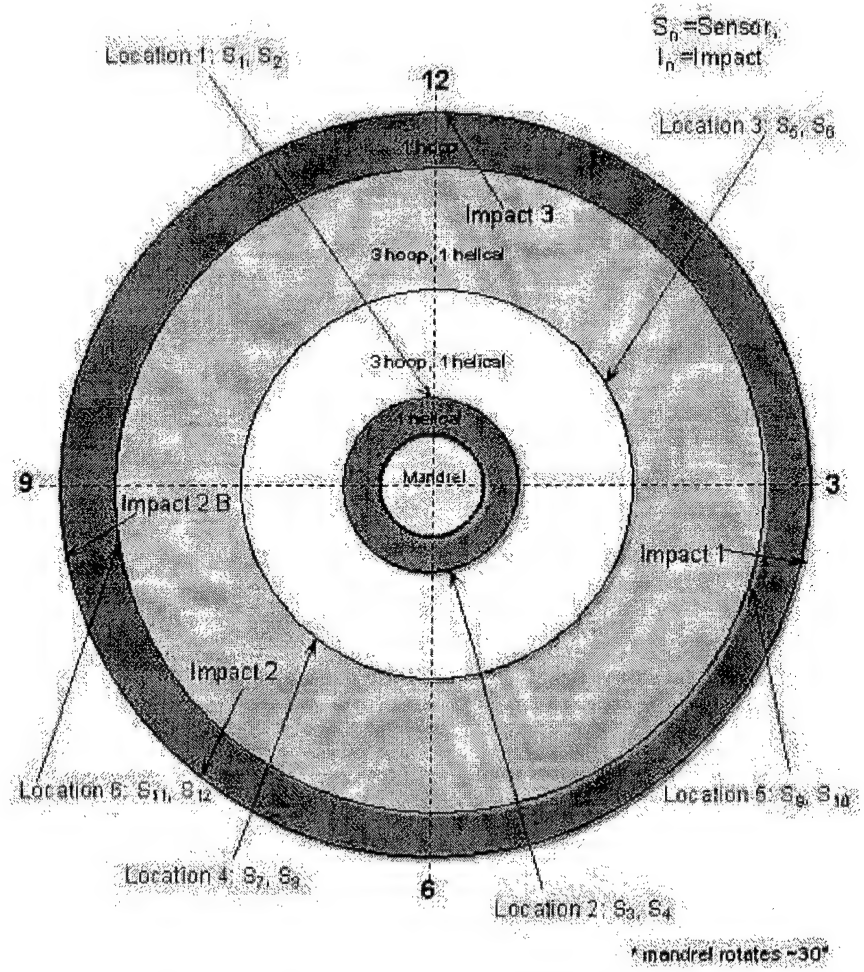

BLUE ROAD RESEARCH

5 ft-lb Impact, Near Sensor # 9

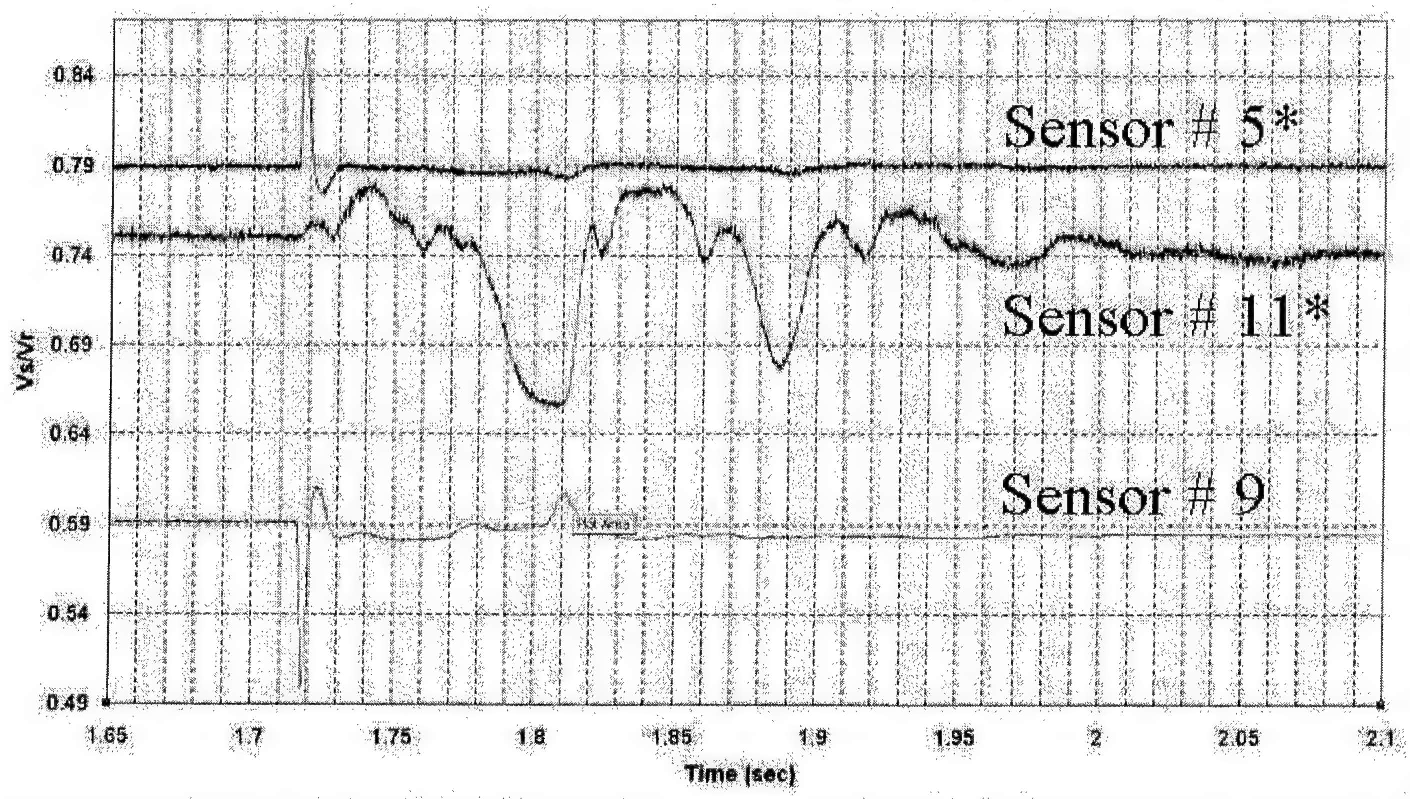

*Sensor 11 is in the top layer on the opposite side of the article from sensor 9, sensor 5 is in the middle layer in ≈ the same position as sensor 9

15 ft-lb Impact (and Bounce) Near Site of Cut Tow Damage and Sensor 7

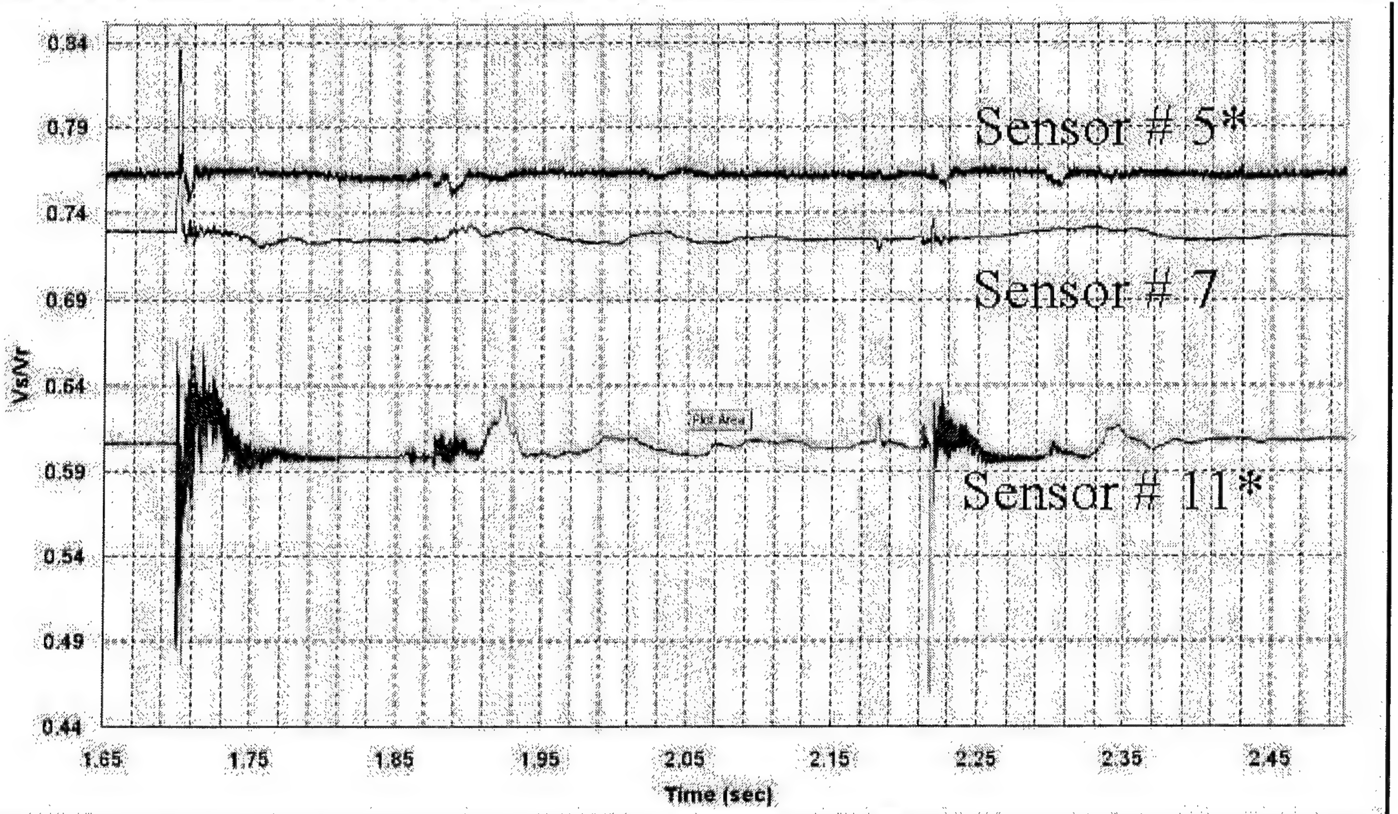

*Sensor 5 is located in the same middle layer as sensor 7 but on the opposite side of the tank. Sensor 11 is on the top layer on the same side of the tank as the impact/sensor 7

BLUE ROAD RESEARCH

Strain Measurements Made During 1st Pressure Cycle

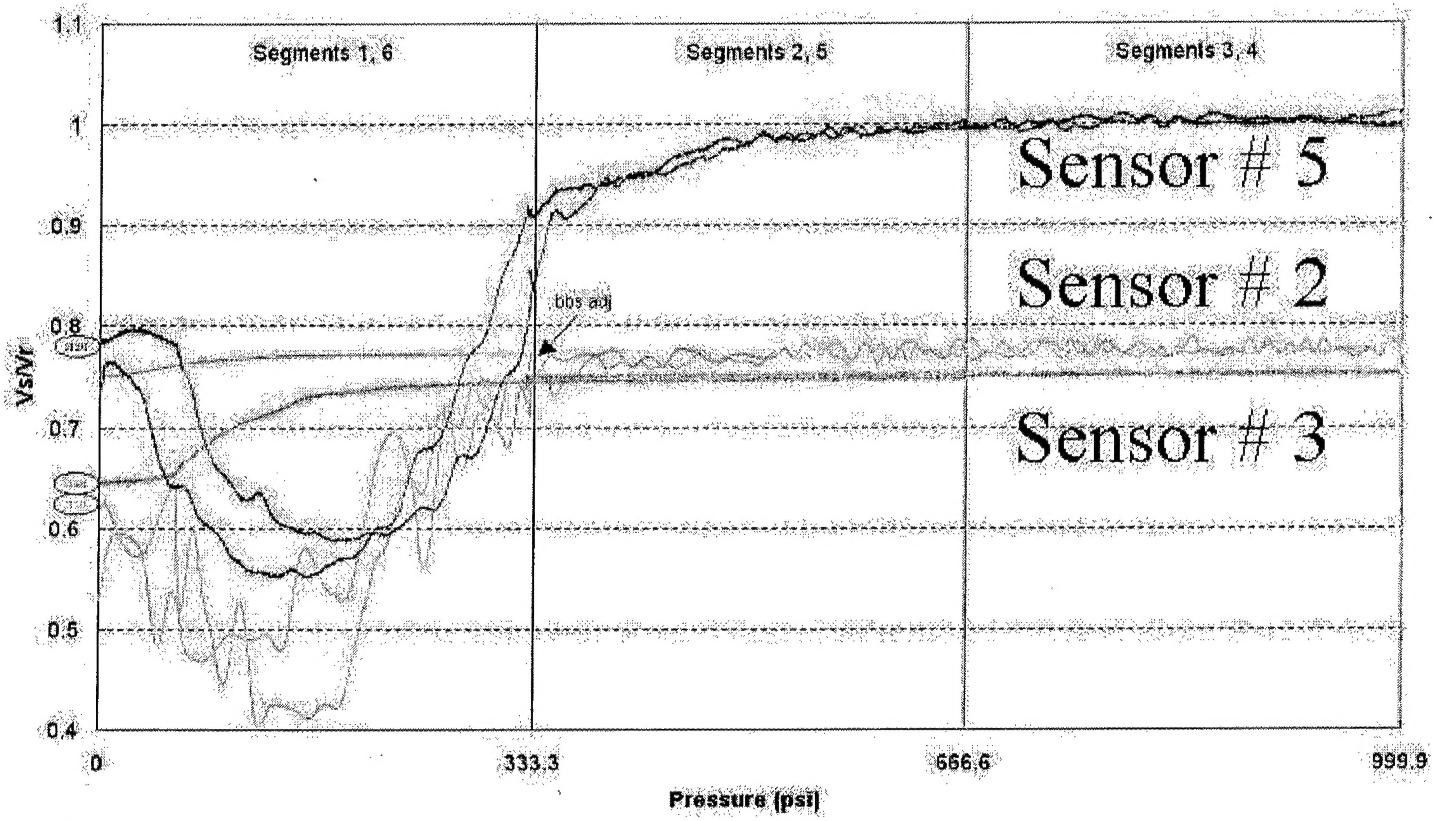

Sensor 2: deepest embedded layer, near Teflon tape flaw
Sensor 3: opposite side of tank, in same layer as sensor 2
Sensor 5: middle embedded layer in same area as sensor 2

BLUE ROAD RESEARCH

Pressure Cycle 3 After the 5 and 15 ft-lb Impacts

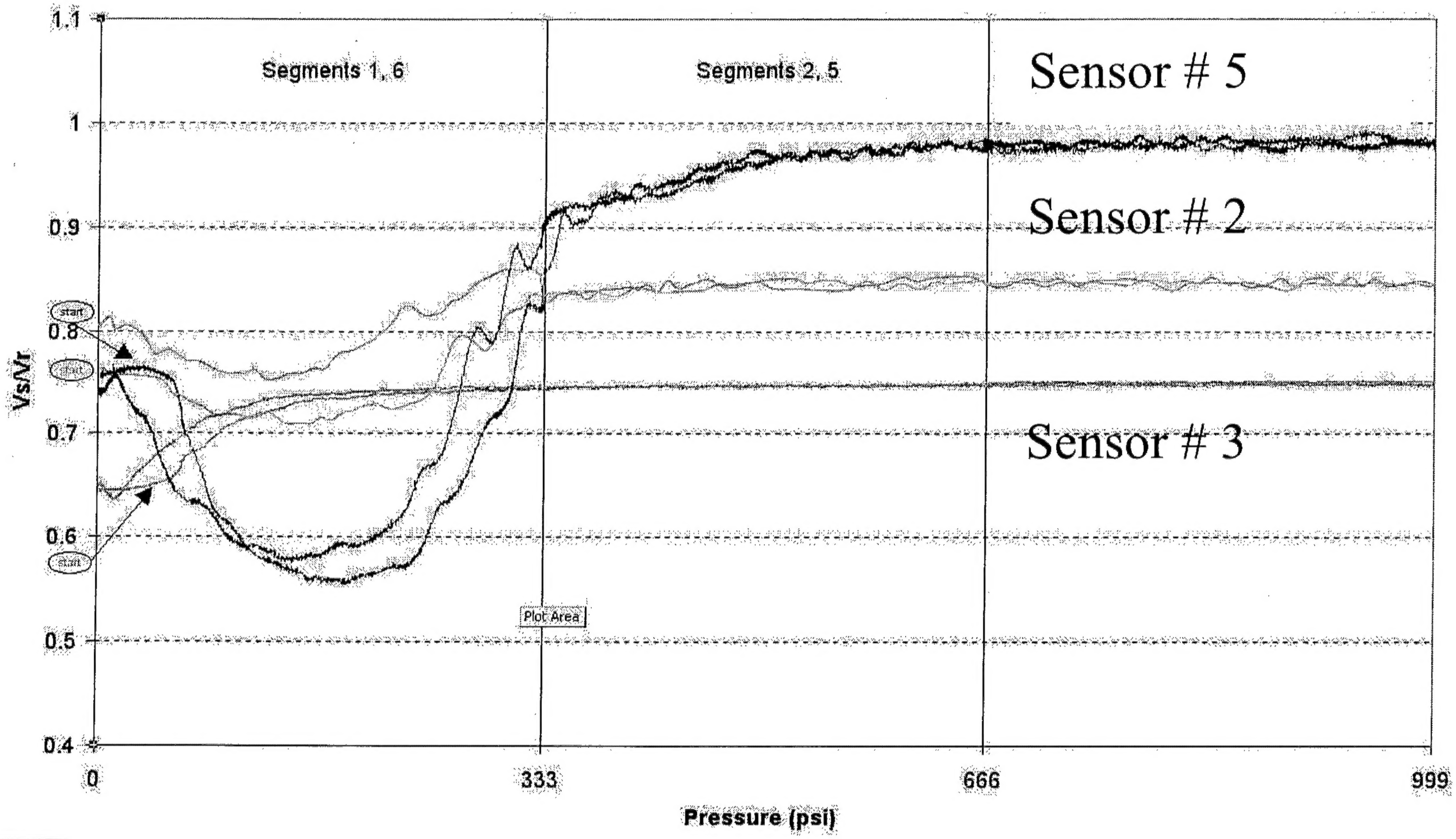

BLUE ROAD RESEARCH

Eddy Current Scan

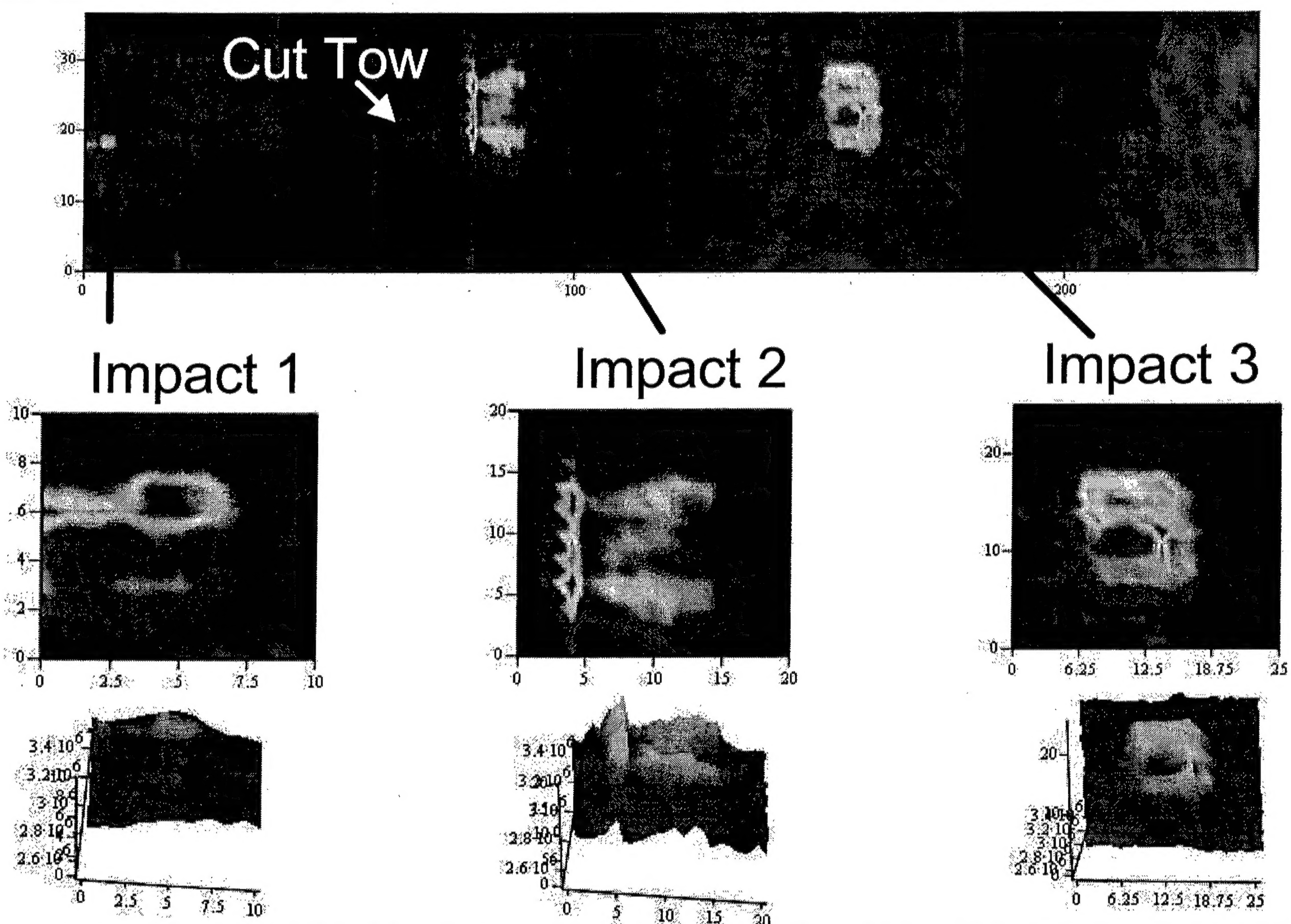

BLUE ROAD RESEARCH

Summary

- Multi-axis fiber grating strain sensors can be used for quantitative damage assessment of adhesive joints

- Cut tow and Teflon tape defects may be detected using multi-axis fiber grating strain sensors

- Quantitative measurements of the evolution of damage due to pressure cycling and impacts can be made using multi-axis fiber grating strain sensors